THE USE OF WATER-COOLING DURING THE CONTINUOUS CASTING OF STEEL AND ALUMINUM ALLOYS

J. Sengupta[†], B. G. Thomas[†], and M. A. Wells[‡]

ABSTRACT

In both the continuous casting of steel slabs and Direct Chill (D.C.) casting of aluminum alloy ingots, water is used to cool the mold in the initial stages of solidification, and then below the mold, where it is in direct contact with the newly solidified surface of the metal. Water-cooling affects the product quality by: (i) controlling the heat removal rate that creates and cools the solid shell, and (ii) generating thermal stresses and strains inside the solidified metal. This work reviews the current state-of-the-art in water-cooling for both the processes, and draws insights by comparing and contrasting the different practices used in each process. The heat extraction coefficient during secondary cooling depends greatly on the surface temperature of the ingot, as represented by boiling water-cooling curves. Thus, the heat extraction rate varies dramatically with time, as the slab/ingot surface temperature changes. Sudden fluctuations in the temperature gradients within the solidifying metal cause thermal stresses, which often lead to cracks, especially near the solidification front, where even small tensile stresses can form hot tears. Hence, a tight control of spray cooling for steel, and practices such as CO_2 injection/pulse water-cooling for aluminium are now used to avoid sudden changes in the strand surface temperature. The goal in each process is to match the rate of heat removal at the surface with the internal supply of latent and sensible heat, in order to lower the metal surface temperature monotonically, until cooling is complete.

Keywords: *Continuous casting, steel, Direct Chill casting, aluminum, comparison, primary cooling, water-cooling, secondary cooling, spray cooling, boiling water cooling curves, Leidenfrost temperature, nucleate boiling, film boiling, temperature profiles, solidification.*

I. INTRODUCTION

Continuous casting processes for both steel and aluminum alloys were developed several decades ago to produce shapes for subsequent semi-fabrication processes like extrusion or rolling. As-cast product shapes include billets (square cross-section with thickness less than ~150-175 mm for steel), thick slabs/ingots (wide rectangular cross-section with thickness between ~50-300 mm for steel, and up to ~500-750 mm for aluminum alloys), thin slabs (thickness between ~50-75 mm for steel), strips (thickness between ~1-12 mm for both steel and aluminum alloys), and rounds/extrusion billets (~500-1000 mm diameter for both steel and aluminum alloys). In recent decades, a dramatic growth of this primary metal processing technology has been realized in both the steel and aluminum industries, owing to a substantial increase in yield, energy savings, and productivity over static casting. However, the technological advancement has taken distinctly different routes for these two metal industries. Over

[†]JOYDEEP SENGUPTA, NSERC (CANADA) Postdoctoral Fellow, and BRIAN G. THOMAS, Professor are with the Department of Mechanical & Industrial Engineering, 1206 West Green Street, University of Illinois at Urbana-Champaign, IL 61801, USA. Contact email: bgthomas@uiuc.edu

[‡] MARY A. WELLS is Assistant Professor in the Department of Metals & Materials Engineering, 309-6350 Stores Road, University of British Columbia, Vancouver, B. C. V6T 1Z4, CANADA. Contact email: mary@cmpe.ubc.ca

the years, the casting procedures for steel and aluminum alloy products have developed distinctive features in terms of casting practices, machinery, and process and quality control methodologies.

The productivity of both processes is controlled by the casting speed, so higher speeds are always sought. However, the casting speed cannot be increased arbitrarily for several reasons[1]. Firstly, the resulting increase in depth of the liquid pool and surface temperature of the strand prolongs the solidification process and increases the cooling requirements. In extreme cases, the structurally weak solid shell may rupture, leading to a "breakout" of liquid metal below the mold, or to excessive bulging if containment is exceeded for larger sections. Secondly, higher casting speeds often lead to cracks, caused by the higher thermal stresses. The practical range of operating speeds at which the casting may be performed is therefore limited and varies with alloy composition and product geometry. For steel slabs, the casting speed increases with decreasing thickness from 0.01 ms^{-1} (for 300 mm blooms) to 0.08 ms^{-1} (for 50 mm thin slabs). Owing to cracking difficulties during startup, aluminum alloy ingots are cast at much lower speeds, increasing from ~0.00075-0.001 ms^{-1}[2] to steady speeds ranging from 0.001-0.003 ms^{-1}[3].

The continuous casting machinery is comprised of the mold and secondary water-cooling systems. These are designed to extract superheat from the incoming liquid metal (~5% of the total heat content in the metal), latent heat of fusion at the solidification front (~20% of total heat content), and heat of phase transformation and sensible heat (~75% of the total heat content) from the solidified metal. However, the cooling system features for casting steel and aluminum alloys are very different, as schematically illustrated by **Figures 1(a)**[4] (for steel) and **1(b)**[5, 6] (for aluminum alloys).

In the conventional continuous (or strand) casting of steel, shown in **Figure 1(a)**, liquid steel flows from the bottom of a ladle into a small intermediate vessel known as the tundish. It leaves the tundish bottom through a submerged nozzle, according to the position of a stopper-rod or slide-gate flow control system. The liquid flow is directed into the mold (usually ~700-1200 mm in length), and freezes a thin shell against the water-cooled copper walls. At steady state, the solid shell exiting the mold forms a stable strand, which has adequate mechanical strength to support the liquid metal core (typically 5~30 m in depth). Motor-driven drive rolls located far below the mold continuously withdraw the strand downward. Many closely-spaced support rolls prevent the outward bulging of the shell due to the ferrostatic pressure arising from the liquid steel core. Water sprays emerge from high-pressure nozzles, which are interspaced between the support rolls and cool the strand during the solidification process. Other strategically-placed rolls bend the shell to follow a curved path and then straighten it flat prior to torch cut-off into individual slabs. This allows fully continuous operation. Start-up of this process is a relatively rare occurrence, and is achieved by inserting a "dummy" bar to plug the mold bottom. Thus, the first steel cast in a sequence can be routinely downgraded or scrapped for defects without incurring a significant yield loss.

The D.C. casting process for aluminum alloys is shown schematically in **Figure 1(b)**. In contrast to the continuous casting process for steel, D.C. casting is only semi-continuous, as the strand is withdrawn vertically for a short length (~10 m) until the process must be stopped and restarted when the cast ingot reaches the bottom of the casting pit. Thus, considerable attention must focus on the initial start-up stage, when defects are most likely to be initiated. To start the process, a bottom block is partially inserted into an open rectangular mold (usually ~100-150 mm in length). Superheated liquid aluminum flows through a launder, down the nozzle spout, through a distribution bag, and into the mold, at a predetermined, time-varying filling rate. Once the molten metal fills the bottom block to a prescribed height, the bottom block and cast ingot are lowered into a casting pit. The aluminum ingot is subjected to cooling by the transfer of heat to the water-cooled aluminum mold over a very short length (~70-90 mm), and to cooling through the contact of chill water with the solid shell after it emerges from the mold cavity. This water emerges from a series of holes, which surround the mold at its base. The defining character of the D.C. casting process is the extraction of heat due to this direct impingement of water on the ingot surface – typically more than 80% of the total heat is removed by

this method under steady state conditions[7]. The thermal field in this semi-continuous process can be considered to develop in two distinct stages. During the start-up, or Stage I, the liquid pool profile and thermal field continuously evolve with time. Finally, during the steady state, or Stage II, the liquid pool profile remains essentially constant or "fully developed", relative to the mold (typically ~200-500 mm in depth depending on the ingot size and alloy composition[3, 8]). Steady state operation is usually achieved within a cast length of ~0.5-1 m.

Some of the contrasting features between the continuous casting of steel and D.C. casting of aluminum alloys can be attributed to the differences between the thermo-physical properties of the two metals. Referring to **Table 1**[9-11], these can be summarized as follows:

(i) The melting temperature of aluminum alloys is significantly lower than steel. As a consequence, continuous casting machines must remove more heat per unit mass of steel and operate in a higher temperature environment than aluminum alloys.

(ii) The thermal conductivity of aluminum alloys is an order of magnitude higher than that of steel. Combined with the slower casting speed (~10x slower than steel continuous casting), this causes faster internal heat extraction, resulting in the relatively short liquid pool in D.C. casting of aluminum alloys mentioned earlier. To avoid cracking the solid strand, D.C.-cast ingots must be cast vertically without bending. This limits the cast length before it must be removed from the casting pit and production restarted for a new ingot. In contrast, the liquid metal pool during continuous casting of steel extends well below the mold. This results in a strand with a liquid-filled shell structure, which can be easily bent and straightened to generate a continuous supply of solidified semi-finished product.

(iii) The thermal diffusivity of liquid aluminum is about 6 times higher than that of liquid steel. This means that liquid aluminum tends to lose its superheat faster than liquid steel, for a given fluid flow pattern. Temperature profiles in the solid aluminum therefore respond faster to changes in surface heat removal.

(iv) The solidification shrinkage experienced by aluminum alloys is almost twice that of steel. Therefore, higher thermal stresses can be generated within the solidification "mushy" zone by aluminum alloys, making hot tear cracks more likely, especially in alloys with long freezing ranges.

(v) The volumetric latent heat of aluminum is substantially less, making initial solidification at the meniscus much faster than in steel.

(vi) The thermal contraction coefficient of solid aluminum is higher than in steel. During initial solidification, the extra contraction of the solid shell causes deeper surface depressions, resulting in a marked reduction in mold heat flow and surface quality problems. Also, the larger thermal contraction during D.C. casting leads to greater macro-deformation of aluminum ingots. One example is the characteristic deformation of the ingot base, called butt curl[5, 12], which develops during startup, especially when cooling water reaches the ingot surface within the base region[13].

This paper was undertaken to compare and contrast the heat transfer phenomena in continuous casting of steel and aluminum alloys, focusing on water-cooling. The implications on quality problems are then discussed. Finally, optimal practices for the control of cooling in both processes are evaluated in the light of these fundamentals.

II. HEAT TRANSFER DURING CONTINUOUS CASTING PROCESSES

Although the continuous casting processes for steel and aluminum have many differences, as just introduced, there are also many similarities owing to the same primary goal of heat extraction from the molten and solidifying metal. The various heat transfer phenomena acting on the surface of the

strand during the continuous casting of steel, and D.C. casting of aluminum alloys are schematically shown in **Figures 2(a)**[14] and **2(b)**[5], respectively. Both processes involve a complex interplay of several heat transfer mechanisms, which include: convection of superheat in the liquid pool due to the momentum of the incoming metal, axial advection and conduction through the moving solid shell, heat conduction from the solidification front to the colder outside surface of the metal, and heat transfer by convection to the mold (referred to as primary cooling), to the cooling water below the mold (referred to as secondary cooling), and to the bottom block (for D.C. casting only during startup).

However, the relative importance of these heat flow mechanisms is different, as evidenced by comparing the Péclet (*Pe)* and Biot (*Bi*) numbers. The Péclet number is the ratio of advective to conductive heat flow given by $Pe = \rho c_p VR / k$, where ρ is density in kgm^{-3}, c_p is specific heat in $Jkg^{-1}K^{-1}$, V is casting speed in ms^{-1}, R is size of the casting in m, and k is thermal conductivity in $Wm^{-1}K^{-1}$. The low typical Pe range for D.C. casting of aluminum, *i.e.* $1.8<Pe<4.5$, indicates that axial conduction is as strong as advection. The Biot number is the ratio of convective to conductive heat flow given by $Bi = hR / k$, where h is the convective heat transfer coefficient active on the strand surface in $Wm^{-2}K^{-1}$, and R is the conductive path length in m. The relatively low value of *Bi* for D.C. casting, *i.e.* $2<Bi<60$[3], indicates that the convective thermal resistance offered by the mold/cooling water contact at the ingot surface can greatly affect the heat transfer in the transverse direction.

In contrast, for continuous casting of steel these numbers are much higher (~1000x for *Pe* and ~10x for *Bi*) owing to the higher casting speed and lower thermal conductivity. This indicates that the conductive component in the axial direction is negligible compared to the advective component, while the thermal resistance offered by conduction through the casting thickness dominates heat transfer in the transverse direction. The Biot and Péclet numbers also indicate the behavior of the liquid core depth profile. For $Bi>10$, the liquid pool shape lengthens almost linearly with increasing *Pe* and is almost insensitive to surface heat extraction rate[15]. This indicates that the pool depth is proportional to the casting speed and inversely proportional to the metal conductivity, as noted earlier. The thickness of the semi-solid (or mushy) zone and the hot tearing susceptibility are also sensitive to the Péclet number[16].

The heat transfer mechanisms discussed above not only control the liquid pool shape, which has important implications for productivity, but also the magnitude of thermal stresses and strains generated in the strand owing to thermal contraction of the metal upon cooling. Changes in the temperature gradient across the solid shell due to an abrupt increase or decrease in the heat extraction rate causes differential thermal expansion in the solidifying metal and the generation of high thermal stress and strain. This can ultimately lead to internal or surface defects, which can severely compromise the quality of the cast product. The following sub-sections discuss the different heat transfer phenomena that occur during continuous casting.

Mold (or Primary) Cooling

Heat is supplied into a water-cooled mold by the continuous flow of incoming liquid metal during the continuous casting process. Heat transport in the liquid pool inside the mold and at the mold/metal interface affects both initial solidification at the meniscus, and growth of the solid shell against the mold. The liquid metal usually enters the mold cavity through a ceramic entry nozzle. The angle and shape of the nozzle ports control the direction and turbulence of the liquid metal jets, which in turn control the flow pattern in the mold. The flow pattern controls stability and oscillation of the meniscus, which governs the surface shape, including the depth of depressions or oscillation marks, and associated defects. The flow pattern also governs the removal of superheat inside the shell where the jet impinges against the solidification front. To decrease the friction between the mold and strand,

a lubricating medium is often added to the mold, which forms either a vapor or liquid layer, which prevents direct contact between the strand and mold walls.

Heat transfer at the metal/mold interface in continuous casting is referred to as mold or primary cooling. It varies with time, or distance down the mold, and can be subdivided into two regions of behavior[17, 18]: (i) mold/metal direct contact, and (ii) air gap cooling, as shown in **Figure 3(a)**. In the beginning at the meniscus, the solidifying metal is in close contact with the mold, and the heat transfer rate is very high. Specifically, peak heat fluxes can exceed 10 MWm^{-2} in steel continuous casting[1, 19] and 1 MWm^{-2} in aluminum D.C. casting[2]. The latter process has smaller values for several reasons. Firstly, the roughness of the cast surface depends on alloy composition, as shown in **Figure 4**, (0.05 mm for AA1050 - 0.45 mm for AA5182 aluminum alloys)[20] and (0.25 mm for low and high carbon steels - 0.65 mm for peritectic grades)[21], and this will impact on the heat flux in the mold. The D.C. cast surface likely has thicker oxide layers with different properties, which would increase the contact resistance of the interfacial gap. In addition, the aluminum shell conducts heat faster away from the peak heat flux region, which is also shorter in length. In steel continuous casting, the newly-formed shell remains in relatively good contact with most of the 700 mm long mold, owing to pressure from the internal liquid pool pushing the weak shell against the mold walls, and intentional tapering of the mold walls to match the solidification shrinkage. In D.C. casting, however, the duration of this initial contact stage is quite brief, ending within 80 mm of mold-metal contact.

Stage (i) ends with the formation of a significant air gap between the metal and mold as soon as the solid shell is strong enough to contract away from the mold faces. In steel continuous casting, this happens only near the corners. In the D.C. casting process, shrinkage of the thick shell away from the un-tapered mold produces gap formation around the entire perimeter. Once the gap has formed, the heat transfer rate is greatly reduced, resulting in a reheating effect within the solid shell. Within stage (ii), heat is conducted away from the shell via a series of thermal resistances[22]: (1) air gap, (2) mold wall, and (3) mold/cooling water interface, which are shown in **Figure 3(b)**[22]. The interfacial gap comprises up to 85% of this resistance [23] and therefore, controls the heat transfer inside the mold.

Figure 5[24] illustrates more of the complex phenomena related to fluid flow and heat transport inside the mold during the continuous casting of steel. The flow pattern and turbulence in the pool is controlled by the nozzle port geometry and submergence depth[25]. Argon gas is often injected to prevent nozzle clogging[25], and the resulting bubbles provide buoyancy that greatly affects the fluid flow pattern. These bubbles can also collect solid inclusions (such as alumina), which enter the metal pool through the nozzle and get entrapped in the solidifying shell, leading to internal defects in the final product[26]. The jets from the nozzle carry superheat, which can sometimes melt through locally thin regions in the solidifying shell and cause breakouts[26]. The jets also carry significant momentum, which controls the flow pattern and affects level fluctuations and meniscus solidification at the top surface. The corresponding flow phenomena during D.C. casting of aluminum are shown in **Figure 6**[27]. Strong and irregular turbulent flow caused by direct or oblique entry of metal can create unfavorable (columnar) grain structures and uneven distribution of the alloying elements[27]. These problems are overcome by surrounding the nozzle in a distribution bag[28], which diffuses some of the jet momentum and encourages a slower, more stable flow pattern that is also influenced by natural convection.

During the continuous casting of steel, heat transfer is complicated by the presence of mold flux. Its source is the mold powder, which is added to the free surface of the liquid steel to provide thermal and chemical insulation from the atmosphere and to absorb alumina inclusions. The powder sinters and melts, spreading over the meniscus and entering the air gap between the steel shell and mold wall[29]. Some of the liquid flux/slag re-solidifies against the cold mold wall creating a solid flux/slag rim (refer to **Figure 3**). Primary cooling at the meniscus is further complicated by the vertical oscillation of the mold, which prevents sticking of the shell to the mold and encourages entrainment of the molten flux into the mold/shell interfacial gap[22]. However, each oscillation cycle

creates a transverse depression in the solidifying shell at the meniscus, called an oscillation mark, shown in **Figure 4(b)**. Pressure from interaction with the flux rim at the meniscus can deepen these marks[30], according to the size of the rim. Unsteady level fluctuations and surface waves due to turbulence can disturb formation of these marks, creating surface defects, such as ripples or depressions in the final product and are potential sites for transverse cracks[22]. Deep oscillation marks increase the local gap resistance, thereby reducing the heat transfer to the mold and retarding the shell growth[21]. The flux layers between the shell and mold wall facilitate uniform and usually lower heat transfer across the interfacial gap, compared with that of lubricating oil used in billet casting, which tends to produce an intermittent vapor gap. Heat transport across the gap naturally depends on the thermal properties and thickness of the flux layers[18]. The gap size in turn depends on the oscillation mark and surface roughness profile, shrinkage of the solidifying shell, mold distortion, and the internal pressure exerted on the shell by the liquid metal[31, 32]. The gap formed by shrinkage of the shell away from the mold walls is largest where it begins at the corners, and spreads across the faces, which further complicates the heat transfer process[31]. The mold walls are routinely tapered to match the steel shrinkage in order to minimize air gap formation and to facilitate primary cooling[33].

It is estimated that primary cooling during continuous casting of steel in the mold removes about 40% of the total superheat, and about 30% of the total sensible heat[11]. The axial heat transfer coefficient typically decreases down the length of the mold from a peak value of 1500-2000 $Wm^{-2}K^{-1}$ at the meniscus to about 600-800 $Wm^{-2}K^{-1}$ [21] near mold bottom. Many strand defects, such as transverse mid face and corner cracks, can be directly attributed to factors that control primary heat transfer in the mold, including oscillation marks, improper mold lubrication, metal level fluctuations in the mold, and improper mold taper[34, 35].

Primary cooling in the mold accounts for only about 20% of the total heat extracted[36] from the solidifying ingot during the D.C. casting of aluminum alloys, but it still has a critical influence on the ingot surface microstructure and roughness[37]. The heat extracted by primary cooling determines the surface temperature of the ingot at the point of exit from the mold. This subsequently influences the mode of boiling water heat transfer (film/nucleate boiling) below the mold[38], as discussed later. The peak heat transfer coefficient reported for aluminum contacting a chilled mold ranges from 2000-4000 $Wm^{-2}K^{-1}$[39]. By comparison, in the air gap, the heat transfer coefficient may be as low as approximately 150 $Wm^{-2}K^{-1}$ in the air gap[40].

In D.C. casting, the molten aluminum quickly freezes at the meniscus to form a thick solid shell, owing to the higher thermal conductivity, thermal diffusivity and contraction coefficient of aluminum, relative to steel. As mentioned earlier, the low Péclet number in D.C. casting allows the chill water below the mold to remove heat from aluminum still inside the mold. Combined with the lack of mold taper, this causes the air gap to form very near to the meniscus and to extend over most of the mold. The extent of the solid shell inside the mold is referred to as the upstream conduction distance (UCD)[3]. If the meniscus level inside the mold is too high (refer to **Figure 7(a)**[41]), the larger UCD, and corresponding longer wider air gap, allows non-uniform reheating of the shell surface to cause surface composition variations due to macro-segregation, and even exudation, where solute penetrates through the local thin regions of the partially solidified shell. Subsequent freezing of solute droplets likely caused the lumps in **Figure 4(a)**. Furthermore, local reduction of cooling rates produces unfavorable microstructures, such as large grain size and dendrite arm spacing[27]. On the other hand, if the meniscus level is too low (refer to **Figure 7(b)**[41]), the smaller UCD can cause the meniscus to freeze. As new liquid flows over the frozen meniscus, a fold is formed and the ingot surface emerging from the mold has a rippled/lapped appearance, such as shown in **Figure 4(a)**. These defects can ultimately lead to transverse cracking during subsequent processing, so an optimum UCD is always desired. Mold flux is not needed to protect the top surface in D.C. casting because the molten aluminum quickly oxidizes to form a protective layer of alumina. Instead, lubricating oil is applied to

prevent sticking and also to reduce the amount of heat that flows through the mold wall[3], as also done in steel billet casting when surface quality is not a concern [3].

To optimize heat transport inside the mold and also control the meniscus level, several strategies have been implemented in the aluminum industry. In open top molds, the metal level is lowered until folding occurs and then increased slightly[3]. Insulating material is placed on hot top molds, and the UCD is allowed to coincide with a fixed point below the insulation. Surface quality has been reported to improve dramatically[3]. A further improvement in controlling the meniscus contact point is achieved by air-assisted hot top mold systems[42]. In the electromagnetic casting process[43], the mold is completely eliminated and electromagnetic force is applied to support the metallostatic head. Lack of contact between the mold and metal removes the problem of air gap formation resulting in uniform cast microstructures. The challenge then becomes maintaining stability of the unsupported meniscus by careful adjustment of the electromagnetic force to balance surface flows.

Another important factor controlling the extent of primary cooling is the effect of the cooling water on temperature and distortion of the mold itself. During the continuous casting of steel, cooling water flowing through the vertical slots in the copper mold extract heat from the mold and simultaneously control its temperature. The hot-face temperature of the mold indirectly affects the heat extraction rate, by altering the properties of the interfacial gap. Mold variables directly control mold temperature, but the effects on primary cooling are more complex. For example, decreasing the velocity of the cooling water lowers the heat transfer coefficient at the cold-face wall of the mold, causing mold temperature to increase[21]. Increasing the temperature of the hot-face wall of the mold may partially melt the slag rim, leading to increased heat extraction from the mold. The effect is counter-intuitive as primary cooling might increase with less cooling water. Impurities in the water can cause deposition of scale on the mold wall near the meniscus, causing mold temperature to increase[21]. If the cold face temperature becomes too high, water may locally boil to form a stable film of air bubbles on the wall. This virtually stops heat removal and causes the mold to become dangerously hot. The impact of mold cooling water on primary cooling during the D.C. casting of aluminum has not been explored, perhaps because the mold cooling water also has an even more important role below the mold. Research has mostly focused on the secondary heat extraction process of direct impingement of water on the hot metal surface exiting the mold.

Water (or Secondary) Cooling

After emerging from the mold, the continuous-cast strand is cooled by direct contact of water with the hot metal surface, as shown in **Figures 2(a) and 2(b)**. This is referred to as secondary cooling. For steel casting, banks of nozzles located between contact rolls beneath the mold spray water to cool the moving metal strand. Usually, the spray nozzles are arranged into banks or cooling zones, assigned to the top and bottom surfaces of particular strand segments[44], as shown in **Figure 8(a)**. The water is forced under high pressure as droplets that form a mist, which continuously impact upon the metal surface. Therefore, secondary cooling between each pair of rolls involves several different heat transfer mechanisms operating in different sub-zones, which are illustrated in **Figure 8(b)**[24]. These are: (i) roll contact cooling, (ii) radiation and air convection from the bare strand surface just in the roll bite just above the spray region, (iii) cooling due to spray water impingement, (iv) water convection cooling just below the spray region, where water runs down the strand and collects in the roll bite. Bulging of the steel shell caused by ferrostatic pressure can affect these heat transfer sub-zones, especially near the roll bite and if the support rolls are spaced too widely apart[45].

For aluminum casting, water jets emerge from holes located below the water-cooled mold and directly contact the metal surface, as shown in **Figure 9(a)**[20]. These jets form a continuous film, which wets the vertical ingot surfaces and rolls downwards. Referring to **Figure 9(a)**[20], two distinct sub-zones can be distinguished on the ingot surface: (a) the water impingement zone, where abrupt

cooling happens due to the direct contact with water, and (b) the streaming zone located below (a), where the heat flux diminishes as the water film loses momentum with increasing distance from the impingement point. The length of the water impingement zone is usually ~10-15 mm, depending on the diameter of water holes at the base of the mold and angle of impingement.

Secondary cooling mechanisms provided by water spray for steel and water film for aluminum have distinctly different characteristics[46], as presented in **Figure 8(c)** and **9(b)**. In spray cooling (**Figure 8(c)**), water droplets impinge onto the very hot steel surface and vaporize instantaneously to create a boundary layer, which prevents the water from wetting the surface. Heat extraction is higher towards the center of the impingement region, where more of the high-speed droplets have enough momentum to penetrate the vapor layer. Extremely irregular flow conditions develop within the vapor boundary layer and it eventually becomes wavy and is thinned out. The short contact times between the spray droplets and the strand surface increase with water velocity, owing to increased water momentum. Thus, the secondary cooling rate increases greatly with spray water flow rate, although it is almost independent of strand surface temperature. In contrast, under film cooling conditions (**Figure 9(b)**), water flows along the surface at a uniform velocity. As a result, the boundary layer of vapor between the water film and the metal surface tends to be thicker and unperturbed. However, as the metal surface cools, the vapor layer breaks down and the water film starts to contact the strand surface. The area of contact increases with decreasing strand surface temperature, and is accompanied by a sudden increase in heat transfer. The cooling process is transient and is difficult to control.

In the continuous casting of steel, the purpose of secondary cooling is to maintain the heat extraction and solidification initiated in the mold with minimal change in surface temperature in order to avoid generating tensile stresses large enough to cause cracking. Only about 50-60% of the total heat content (including superheat, latent heat, and sensible heat) is removed by secondary cooling[47]. However, this heat transfer process is critical in D.C. casting as the chill water extracts about 80% of the total heat content during the steady state regime below the mold (the term "secondary" appears to be misplaced for the D.C. casting process while referring to cooling by chill water that originates in the mold!).

The extraction of heat by cooling water is quite complex for both water spray and film cooling conditions because it is governed by water boiling water phenomena[48] which depend greatly on temperature. As shown in **Figure 10**, four mechanisms of heat transfer[48] can be distinguished when cooling water comes in contact with a hot metal surface. In order of increasing surface temperature, they are:

Convective cooling at temperatures lower than 100°C – In this regime heat transfer occurs via natural convection currents in the water film adhering to the metal surface, and the heat transfer coefficient is very low.

Nucleate boiling between 100°C – burnout temperature – As the surface temperature increases, bubbles of water vapor form on the metal surface, break off and flow in the water film, and eventually escape from the free surface. The intensity of bubble formation and breakaway continues to increase as the surface temperature rises. This effect encourages good circulation in the water film causing the heat transfer coefficient to increase rapidly until it reaches a maximum (referred to as the burnout point). The burnout temperature is about 200^{o}C, and increases with increasing water flow rate.

Transition boiling between burnout and Leidenfrost temperatures – Beyond the burnout point, the bubbles start sticking to the metal surface and a layer of vapor begins to form, which cuts down the circulation of heat. The heat transfer coefficient decreases sharply with increasing temperature, as the vapor film continues to cover more of the metal surface, with ever-decreasing amounts of metal surface exposed directly to water. When the metal surface is fully covered by a stable vapor film, the heat transfer coefficient associated with the boiling curve reaches a minimum, which is referred to as the Leidenfrost point. The Leidenfrost temperature is about 700-1000^{o}C for steel and 300-500^{o}C for aluminum.

Film boiling at high temperatures (> Leidenfrost temperature) – At temperatures above the Leidenfrost point, heat is transferred by conduction through the stable vapor film. The heat transfer coefficient does not change much with temperature and is very low compared to that at the burnout point.

Two important points characterize the boiling curve in **Figure 10.** They are: (i) the burnout temperature, which indicates the maximum heat flux (and heat transfer coefficient), and determines the maximum ability of the water film to cool the metal surface by nucleate/transition boiling, and (ii) the Leidenfrost temperature, which indicates the change in heat transfer mode from transition to vapor film boiling. Due to the strong co-relationship between the heat transfer coefficient and the surface temperature, heat extraction rates by secondary cooling can change rapidly with time and location near the Leidenfrost temperature. High heat transfer rates associated with nucleate boiling can cause surface temperature to decrease rapidly. In contrast, the low heat transfer rates associated with film boiling can allow surface temperature to increase. As a result, abrupt changes in the metal surface temperature can occur as the boiling phenomena is shifted from nucleate to film boiling and *vice versa,* depending on whether the Leidenfrost temperature is exceeded or not. Also, extreme variations of cooling can occur simultaneously at different locations on the metal surface, depending upon the local boiling behavior.

To optimize secondary cooling, the heat transfer rate from the metal surface should produce a stable surface temperature that decreases monotonically. Film boiling is deliberately promoted during the secondary cooling process for the continuous casting of steel, in order to avoid the unstable surface temperatures and heat extraction rates that accompany nucleate/transition boiling, if the steel surface temperature drops too low. However, during the D.C. casting process, nucleate boiling is desired on the ingot surfaces during secondary cooling, in order to achieve high enough heat extraction rates under steady-state operations. During start-up, however, it is a common industry practice to deliberately maintain a lower water flow rate in order to keep the ingot relatively hot for long enough to avoid intense cooling and stress build up. This complicates the secondary cooling, as a portion of the water curtain may be ejected away from the ingot surface due to the formation of a stable film boiling layer beneath it. The heat transfer rate is significantly lower within the region of water ejection, as there is little or no contact of the water film with the ingot surface. The result is a region with greatly reduced cooling at the hottest portion of the ingot surface below the impingement zone. As the ingot surface cools, however, the film boiling switches to transition and then to nucleate boiling. The water curtain is able to travel further down the ingot surface before it is ejected. Eventually, the surface is no longer hot enough to sustain film boiling; the stable film layer region collapses, and the cooling rate increases. The entire surface then has a stable water curtain with nucleate boiling heat transfer. This process is illustrated schematically in **Figure 11(a)**[49]. The film boiling area appears as a visible "dome" on the ingot surfaces, with a parabola shaped steam barrier profile demarcating the nucleate/transition and film boiling heat transfer zones. This visual manifestation of water ejection, which is observed on the ingot vertical faces during the start-up phase, is illustrated in **Figure 11(b)**[50].

The various heat transfer mechanisms associated with secondary cooling during continuous casting of both steel and aluminum are important because they determine the temperature gradients that develop inside the solidifying strand. Thus, they significantly influence the development of internal thermal stress/strain below the mold, and can aggravate defects generated inside the mold or introduce new defects. Quality problems related to secondary cooling will be discussed in Section III.

Radiative Cooling during Continuous Casting of Steel

Beyond the spray zone region, the heat transfer process simplifies to radiation and natural convection. The smaller cooling rate of radiative cooling results in reheating of the solidified strand, which causes the strand surface to expand. If the surface reheats too much before complete

solidification, then plastic deformation of the hot austenitic shell and semi-solid core may not be able to accommodate this expansion. This may cause sub-surface hot-tear cracks to form at the solidification front[14]. These cracks can cause internal segregation defects, or they may propagate through to the surface during later processing, such as rolling.

Ingot base cooling during the D.C. Casting of Aluminum Alloys

Secondary cooling also plays an important role in cooling the ingot base during the beginning of the start-up phase of the D.C. casting process. As the liquid metal enters the bottom block, the initial rate of heat transfer from the molten metal to the cold bottom block is extremely high. After a very short time, a small gap at the interface forms due to solidification shrinkage and the rate of heat transfer drops. This gap remains relatively small until the ingot begins to withdraw from the mold and the base experiences a large macroscopic thermal distortion, called "butt curl". This is aggravated by the slow cooling of the base, owing to the large gap and lack of water, combined with high thermal contraction of the vertical sides of the ingot, which experience higher heat extraction from the direct contact of a stable curtain. As the base continues to deform (or curl), water flowing down the sides may enter the bottom gap (water incursion) and enhance the heat transfer from the ingot base[51, 52]. This in turn will influence further deformation of the base. The details of the important interfacial heat transfer processes active near the base of the ingot are schematically shown in **Figure 12**[5].

Strand Cooling Behavior

Figures **13(a)**[24] and **(b)**[5] compare typical surface temperature profiles along the strand length observed during the continuous casting of steel and aluminum alloys, respectively. **Figure 13(b)** also compares two aluminum ingots, produced by D.C. casting at different cooling rates (lower water flow rates were used for the hot cast). The primary and secondary cooling heat transfer regimes can be easily identified in the cooling curves of both processes (refer to the cold cast in **Figure 13(b)**). For steel, the extent of primary cooling is important, as it results in a temperature drop of ~250 °C, whereas for aluminum the initial drop in the mold is ~100 °C. This is followed, by reheating caused by the long air gap. Below the mold, the temperature during the continuous casting of steel varies over ~100 °C over each roll pitch, as shown in **Figure 13(a)**. Near the top of the caster, the greatest surface temperature drop occurs beneath each spray jet, while a tiny dip occurs at each small region of direct contact with a contact roll. Lower in the caster, the growing ferrostatic pressure increases the local heat extraction during roll contact, which makes the relative size of the spray and roll-contact dips become closer. In contrast, during the D.C. casting process, **Figure 13(b)** shows that aggressive cooling from direct impingement of water at a high flow rate onto the metal surface, causes the ingot surface to cool monotonically by ~450-500 °C in only 300mm. With less water, the hot cast did not achieve sufficient cooling at the impingement zone, allowing the surface temperature of the ingot to exceed the Leidenfrost temperature. As a result, the heat transfer was in the film boiling range (refer to **Figure 10**), such that the rate of heat transfer was low and kept the solidifying shell dangerously hot near the solidus temperature for a long time. This also caused the macro-deformation of the ingot base to decrease from ~50 mm for the cold cast to ~6 mm for the hot cast.

III. QUALITY PROBLEMS RELATED TO SECONDARY COOLING

One of the most important considerations during the continuous casting process is the capability of attaining a defect-free slab or ingot. The quality issues of most concern are: (i) hot tearing and cold cracking, and (ii) dimensional control (e.g. bulging of the steel shell and butt curl for aluminum ingots). These problems are directly attributed to tensile mechanical and thermal stresses/strains

generated during the casting process. The variety of crack defects that affect continuous cast steel slabs and D.C. cast aluminum ingots are shown schematically in **Figures 14**[53] and **15**[54] respectively. Mechanically generated tensile strains, such as caused by inadequate mold lubrication or bending/straightening of the strand, usually act in the longitudinal direction and cause transverse cracking. During the casting process, rapid cooling can result in steep temperature gradients in the solidifying shell that can generate thermal strains as the shell expands and contracts. Sudden localized cooling can introduce tensile strains at the surface, whereas reheating can generate tensile strains at the solidification front. Thermals strains act predominantly in the transverse direction and are responsible for causing longitudinal cracks. Cracks can form if the generated tensile strain locally exceeds the strain-to-fracture of the metal. In steel, different regions of low ductility have been reported[53]. The most important one lies within ~50 °C of the solidus temperature, and is responsible for "hot tear" cracks. Aluminum experiences a similar rapid loss in strength and ductility between the solidus temperature and the coherency point (*i.e.* the temperature corresponding to about 90% solid fraction)[55]. Other mechanisms involving sulfide, oxide, and nitride precipitates at the grain boundaries operate in steel at lower temperatures, between ~700 and 900 °C[34, 56], and cause intergranular cold cracks.

Most cracks in steel slabs and billets are hot tears, due to the zone of low ductility near to the liquid front. Internal cracks are often seen near the corners, at the centerline or diagonally between opposite corners. Surface cracks can appear near both the midface or corner regions. Some cracks form below 900 °C during the straightening of the shell have been attributed to the embrittlement caused by precipitation of AlN near the grain boundaries[56]. In aluminum ingots/billets, hot tears or "pre-solidification" cracks can also form near the solidification front, when a tensile stress is imposed across partially solidified grains, and the surrounding liquid cannot fill the gap between the grains. Hence, these cracks are always inter-granular. In contrast, cold cracks in aluminum ingots are initiated at temperatures below the solidus due to extremely high thermal stresses, and are always trans-granular.

Brimacombe *et al*[47] have summarized the causes of cracking problems in continuous cast steel**.** Improper secondary cooling practices contribute to many of these. Excessive spray cooling and/or insufficient spray length lead to surface reheating, which induces tensile stresses beneath the surface, including the solidification front. This can cause internal cracks such as midway cracks in billet casting. Unsymmetrical cooling at the billet corners induces distortion and diagonal cracks. Excessive spraying of water can lead to rapid cooling and large tensile strains at the surface of slab castings, which can open up small cracks formed in the mold. However, insufficient spray cooling below the mold can allow the slab to bulge out if the surface becomes too hot. This can lead to several defects, such as triple point cracks, midface cracks, midway cracks, centre-line cracks and centre segregation, as shown in **Figure 14**. Transverse surface and corner cracks begin in the mold, but can be open up by axial tensile stresses induced by spray cooling in slab casting, when the surface temperature is within the low-ductility range of 700-900°C. Secondary cooling practices that lead to excessive surface temperature fluctuations also aggravate these cracks, especially in this critical temperature range.

The thermal stresses and strains generated in the ingot during the transient start-up phase of D.C. casting process can initiate hot tears and cold cracks, especially in high strength aluminum alloys[57]. As shown in **Figure 15**, hot tears generally form between the quarter points of a rectangular ingot and may not be visible on the ingot surface. Cold cracks also originate at the ingot base and are located in the centre half of the ingot width. High casting speeds tend to cause hot tears and low casting speeds increase the risk of cold cracks[3]. The formation of hot tears has also been linked with the frictional forces between the ingot and mold (which is related to mold cleanliness)[41], and the variability in cooling conditions during the transient start-up phase[58]. In addition to cracks, thermal stresses related to secondary cooling also generate macro-deformation of the ingot base or butt curl especially during start-up. As reported by Droste and Schneider[12], the production problems related to

butt curl include: run outs of the melt, cold shuts, reduced rigid standing (instability) of the ingot on bottom block, and low recovery rates. Ultimately, if the magnitude of butt curl is excessive, the ingot bottom may have to be sawed off.

IV. FUNDAMENTAL INVESTIGATIONS OF WATER COOLING PROCESSES

Primary Cooling

Many fundamental experiments have been conducted to quantify convective heat transfer in confined channels, and are summarized with empirical correlations[59, 60]. These relations have been applied to the continuous casting of steel, to quantify heat transfer in the mold. The heat transfer coefficient between the sides of the water channels in the mold and the cooling water is calculated assuming turbulent flow through an equivalent diameter pipe, such as described by the following relationship[60]:

$$h_w = \frac{k_{water}}{D}\left[5 + 0.015\, Re_{waterf}^{c_1}\, Pr_{waterw}^{c_2}\right] \qquad [2]$$

where D is the equivalent diameter of the water channel, Re_{waterf} is the Reynolds number at average of mold cold face and cooling water temperatures, Pr_{waterw} is the Prandtl number of water at the mold cold face temperature, c_1 and c_2 are empirical constants. Other similar relationships are discussed elsewhere[24].

Increasing water flow in the mold increases the heat transfer rate and thereby decreases the mold temperature, leading to less mold distortion and fewer surface cracks. As discussed previously, the effect on mold heat flux is indirect, because mold heat flux is controlled mainly by the interfacial gap and thickness of solidifying shell. This relationship is well appreciated in continuous casting of steel, but has received little attention in D.C. casting molds.

Secondary Cooling

Experiments have been conducted to quantify heat transfer from water cooling and to establish boiling water curves (refer to **Figure 10**) in controlled laboratory experiments on small steel[47, 61-66] and aluminum[20, 49, 67-74] samples, in plant measurements of secondary cooling in the continuous casting of steel[75], and in D.C. casting of aluminum[76-79]. Generally, empirical relationships are developed by applying inverse heat transfer analysis to the measurements recorded by thermocouples embedded in the plate or casting. **Figure16**[20, 47] compares typical boiling curves for steel and aluminum alloys obtained from such laboratory studies. Although the basic features of the boiling curves for the two systems are the same, the magnitude of maximum heat flux and Leidenfrost temperatures will differ due to the differences in thermo-physical properties[46] of the two metals as well as surface effects such as oxide layers and surface roughness. A heat input coefficient can be defined by the relationship $b = \sqrt{\rho k c_p}$, which characterizes the heat transport to the metal/water interface. The value of b for aluminum is ~1.5 times greater than steel, indicating that heat flux can cross the interface more easily for aluminum than for steel.

Studies on secondary cooling and the boiling water curve for the continuous casting of steel reveal the following observations:

1. Typical values of maximum heat transfer coefficient measured by different researchers[63, 65, 75] lie between 2.0-3.0 $kWm^{-2}K^{-1}$ at the burnout temperature of ~500-700 °C.

2. Within the desired surface temperature range of 900-1200 °C for spray cooling, the surface temperature of the strand has little impact on the spray heat transfer coefficient. This relative lack of dependence clearly indicates that the heat transfer mechanism is dominated by the convective heat transport occurring between the surface of the casting and a stable film of steam adhering to it (film boiling).
3. Within the film boiling regime, the spray heat transfer coefficient has a strong correlation with the water flow rate, as represented by the following empirical relationship[65]:

$$h_{spray} = A\dot{W}^{c} \qquad [1]$$

where h_{spray} is the spray heat transfer coefficient (in $Wm^{-2}K^{-1}$), A and c are fitting parameters, and $\dot{W}$ is the water flow rate (in $lm^{-2}s^{-1}$). Typically, A is 0.45 to 0.75, and c is 0.5-1.0[47].

4. Increasing the discharge velocity of the spray droplets increases their momentum to break through the vapor layer, which suppresses stable film boiling, and thus increases the heat transfer rate[63].
5. The Leidenfrost temperature is ~1000 ^{o}C and increases sharply with increasing water flow rate, for the same reason.
6. Increasing the temperature of the spray water has little influence on the heat transfer coefficient, although one correlation shows a slight decrease[65].
7. The spray nozzle orientation has a small but important effect on the heat transfer coefficient[63]. Specifically, upward spraying is 15% less than downward spraying. Heat transfer coefficient decreases greatly with distance from the impingement point. As spray nozzles are oriented perpendicular to the strand surface, this decrease is roughly symmetrical.

From the secondary cooling studies conducted for D.C. casting of aluminum alloys, the following observations can be made:

1. There is a general agreement between different measurement techniques that the maximum heat flux is between 1-5 MWm^{-2}, and the maximum heat transfer coefficient lies between 40 and 50 $kWm^{-2}K^{-1}$. The corresponding burnout temperature is ~200-250 ^{o}C.
2. Fundamentally, the operating temperature range of 220-620 ^{o}C is wider than for steel casting, extending down to the burnout temperature, so the ingot surface temperature has more effect on the heat transfer.
3. The Leidenfrost temperature is ~250-350 ^{o}C and increases with increasing water flow rate, in the same way as observed for steel. The heat transfer coefficient at the Leidenfrost temperature is very sensitive to water flow rate at low flow rates. Thus, water flow rate determines whether stable film boiling or water ejection will occur during start-up of D.C. casting. The Leidenfrost temperature can also be influenced by the water quality as well as the water temperature[70].
4. The oblique orientation of the water nozzle used in D.C. casting greatly affects the heat transfer. Because flow is directed downward along the ingot surface, the heat flux varies greatly with distance above or below its maximum at the impingement point. It drops significantly in the region of back flow above the impingement point. It decreases only gradually with distance below the impingement point as the water film loses momentum, and can be ejected from the surface by the formation of a stable vapor barrier.
5. The rate of heat extraction is a strong function of metal surface temperature. This is shown in **Figure 17**[20] as a function of temperature at the impingement point and in the streaming zone. This figure shows that the heat flux also depends strongly on the initial temperature of the surface when water is first added, which affects the transient co-evolution of the water layer and the metal surface temperature.

6. Under transient conditions, the rate of heat extraction has also been found to be influenced by alloy thermal conductivity, with higher conductivity material producing higher maximum heat fluxes for a given flow rate and surface temperature[20].
7. The morphology of the ingot surface emerging from the mold has a significant impact on the boiling curve behavior; with rougher surfaces exhibiting higher heat transfer rates[20].

Model Applications

The heat transfer relations obtained from experimental measurements described in the previous section allow the study of thermomechanical behavior in continuous casting processes using mathematical models. These relations can be implemented as Cauchy type boundary conditions into finite-difference (FD) or finite-element (FE) based computational models to describe the cooling processes. These models can then predict the evolution of temperature, shell thickness, stress, and strain in the strand as it is cooled first in the mold and then during the secondary cooling zones. Predicted results from some of these models are presented here to provide further insight into the heat transfer phenomena acting during the continuous casting of steel and aluminum. For example, the distribution of heat removed during the continuous casting of steel can be calculated from a 1-D FD model, CON1D[24]. **Figure 18** shows the heat removed per unit area of the shell surface at different distances along the process. Most of the superheat is removed from the molten steel either inside the mold or near the mold exit. The total heat extracted per unit area of shell surface is similar on the wide and narrow faces. However, the narrow faces extract a larger fraction of the superheat because the bifurcated nozzles used in slab casting direct the superheat jets of molten steel onto the narrow faces. Secondary cooling is responsible for extracting the latent heat and some of the sensible heat from the solidifying shell. The latent heat is almost twice as large as the sensible heat extracted. Similar trends can be expected in the case of D.C. casting of aluminum.

The shell thickness predictions from a 2-D[45] and a 3-D[2] FE based thermal model for casting steel and aluminum are shown in **Figures 19** and **20** respectively. Profiles at mold exit and in the secondary cooling are compared. Temperature gradients through the shell are linear at mold exit. The shell thickness at mold exit is ~20 mm for a typical steel, as shown in **Figure 19**, and its surface temperature drops to 70% of the melting (liquidus) temperature, T_m in absolute degrees (K). In contrast, **Figure 20**, shows that during the D.C. casting of aluminum, the solidifying shell may exit the short mold relatively hotter at 85% of T_m. This may leave the shell in a mushy state if the solidification range of the alloy is large, such as ~100 °C for an AA5182 alloy. Shrinkage of the surface caused by subsequent cooling of the mushy shell by chill water can force the exudation of inter-dendritic liquid droplets, and result in a very rough cast surface, as shown in **Figure 4(a)**. For an AA1050 alloy, the solidification range is <20 °C, so the surface appearance is much smoother.

Inside the mold, the interfacial gap offers most of the resistance to heat extraction. However, beyond the mold exit, the gap does not exist, and the resistance offered by the thickening shell in the secondary cooling zone becomes the rate-limiting factor in the process of heat removal from the strand for both continuous casting processes. It is, therefore, desirable that the secondary cooling process avoids any sudden increase or decrease in the surface heat extraction rate, in order to maintain a linear temperature gradient and avoid surface temperature variations that can generate local thermal strains and cracking problems. **Figure 19** shows the predicted temperature distributions through the shell thickness in the secondary cooling regime for continuous casting of steel between a set of roll pitches. The steel shell is shown to experience rapid changes in the surface heat extraction rate while moving beneath the contact rolls, or moving between regions of intense and less-intense spray cooling. This greatly changes the thermal fields close (~10 mm) to the surface. Intensifying the spray cooling does not improve the rate of solidification, as indicated in **Figure 19** by the almost unchanged linear temperature gradients deep inside the shell. It does, however, cause surface temperature variations that

generate high local thermal strains near the shell surface that can aggravate cracking problems. Sharp drops in surface temperature can generate surface cracks, while the subsequent sharp increases can extend sub-surface cracks. Thermal cycling near the surface around the Ar3 temperature of steel is particularly dangerous because it encourages precipitation of detrimental phases such as AlN and large internal stresses due to volume changes associated with the austenite-to-ferrite phase transformation.

During the start-up phase of the D.C. casting process, the aluminum shell reheats below the mold, as seen in **Figure 20.** This indicates the presence of a stable film boiling front on the rolling face, which reduces the heat transfer coefficient and delays solidification. This effect is clearly indicated in **Figure 21**, which shows temperature contours predicted[2, 5, 80] along the vertical faces of the ingot during the start-up . A steam barrier exists on the vertical faces 20 mm below mold exit owing to the ejection of water film (accompanied by generation of steam) from the ingot surface and along the barrier where the temperature is greater than Leidenfrost temperature. This profile quantifies the schematic in **Figure 11(a)** and shows how the centers of the rolling and narrow faces of the ingot remain at a high temperature for a longer period of time than the ingot corners. This creates hot spots with high tensile strains just beneath the shell surface at the center of the vertical faces, which explains the initiation of hot tears that have been observed at this location. These observations underline the necessity for optimal design of the secondary cooling processes during the continuous casting of both steel and aluminum alloys, which ensure monotonic cooling of the shell, and avoid the initiation and propagation of crack defects.

V. OPTIMIZATION OF WATER COOLING

From the previous discussion, it is evident that water cooling plays a critical role during the continuous casting of steel and the start-up phase of the D.C. casting process for aluminum alloys. Hence, optimizing the parameters that control the cooling process is necessary to generate defect free castings. Mold geometry and operating variables can be designed to control the hot face temperature of the mold at the meniscus, in order to control primary cooling of the shell. The water channels in steel continuous casting molds are routinely configured to optimize heat transfer between the cooling water and mold faces. For example, reducing the channel depth, increasing the spacing and decreasing the width of the water channels leads to higher hot face temperatures[21]. Hot face temperature also decreases with higher water velocity. Some operations adjust water velocity online in order to control mold hot-face temperature.

The task of optimizing secondary cooling is easier for steel continuous casting than for D.C. casting, because cooling is governed by film boiling phenomena so the heat transfer coefficient is relatively independent of the strand surface temperature. Relationships describing the variation of heat flux with nozzle type, nozzle-to-nozzle spacing, spray water flow rate, and distance of the spray nozzles from the strand surface are given in the literature[47, 63, 75, 81-83]. Under steady state conditions, spray practices can be designed to achieve cooling conditions that prevent defects. Specific techniques include "plateau cooling"[66] and air-water mist cooling[84, 85]. The purpose of plateau cooling is to keep the surface temperature of the strand in the spray cooling zone always above 700°C, and to avoid reheating from below this temperature. This procedure can prevent longitudinal, mid-face cracks, which are associated with the loss of ductility in steel at temperatures between 700-900°C. Air-water mist cooling has helped to provide more uniform cooling in both the casting and transverse directions, and hence avoids cracks by minimizing the localized temperature fluctuations caused by the undercooling and overcooling associated with water droplet spray jets. Furthermore, automatic control systems are available in the industry[44, 86] to adjust the sprays according to changes in casting speed and thereby optimize secondary cooling conditions for transient conditions as well. These control systems make use of online computational models to ensure that each portion of the shell experiences the same cooling conditions.

Unfortunately, in the case of D.C. casting, relatively little fundamental work has been done to optimize water-cooling phenomena to control the final ingot quality. Despite increased use of automation, the control of cooling conditions during start-up is difficult due to the many complex parameters and their inter-related effects on ingot cooling. The large number of casting parameters that affect cooling are shown in **Figure 22**[87]. A significant part of the problem to develop a fundamental approach to optimize the transient start-up phase is that the mold, the chill water, and the bottom block simultaneously cool the ingot surfaces. The combined inter-play of primary and base cooling conditions determine the surface temperature of the ingot emerging from the mold, which in turn governs the boiling water-cooling conditions (film/nucleate boiling) that dictate the secondary cooling phenomena. The trend in the aluminum industry has been to control heat transfer by varying the bottom block filling rate, casting speed, and water flow rates during the start-up phase. Because the evolution of butt curl is directly linked with the amount of thermal stress generated in the ingot, attempts have been made in the industry to minimize the amount of curl by reducing the intensity of cooling during the start-up phase. It has further been suggested that combining low cooling water volume with high casting velocities during startup can reduce base deformation for some alloys [12]. If carried too far, however, these practices can cause extremely high local surface temperatures that can lead to extreme butt shrinkage and dangerous casting situations. Butt curl can also be reduced by solidifying a thick bottom shell, which bends to a lesser extent upon direct impingement of water. This can be achieved by appropriate bottom block design[88] or by using longer filling times[89]. Additional state-of-the-art water cooling systems include Alcoa's CO_2 injection[90], Wagstaff's Turbo process[91], and Alcan's Pulse Water technique[92]. Both the Alcoa and Wagstaff techniques use gases to promote film boiling. The gas bubbles in the water film quickly adhere to the ingot surface, generating an insulating layer that reduces the heat transfer coefficient. The Alcan process applies rotary valves to turn the cooling water on and off during the start-up phase. Thus, the average heat flux is lowered and the surface temperature of the ingot becomes high enough to trigger film boiling.

With the development of sophisticated commercial finite element codes and more powerful computers, mathematical models based on fundamental principles can be developed to predict the temperature distribution and stress/strain fields in the solidifying strand during the continuous casting process. This approach can minimize the immense experimental efforts traditionally required to optimize the process. To achieve this, it is critical that these mathematical tools capture all of the complexity of the physical phenomena active during the industrial process. Such models validated by industrial measurement can prove to be powerful tools for process optimization. Also, these thermal models coupled with a stress model and an appropriate hot tearing/cracking criterion can be effectively used to develop permissible process windows for casting defect-free products.

Over the past several decades, mathematical modeling has been extensively used in the steel industry to control both the primary and secondary cooling processes. Models such as CASIM, DYNCOOL, and DYSCOS have been adopted by the industry for online process control[44]. The Continuous Casting Consortium at the University of Illinois at Urbana-Champaign have developed CON1D[24] and CON2D[93] programs to study the fundamentals of the complex but industrially-relevant phenomena in the mold and spray cooling regimes. Several industries and universities have formed consortiums to develop thermomechanical modeling tools to design and optimize the D.C. casting process using finite-element packages such as MARC[94] (at Hoogovens, Netherlands and Péchiney, France), ABAQUS[94] (at EPFL-Lausanne, Switzerland), and ALSIM/ALSPEN (at Institute for Energy Technology, Norway)[36, 95]. National laboratories in the United States (Albany Research Center, Oregon, Argonne National Laboratory, Illinois, and Oak Ridge National Laboratory, Tennessee), and University of Kentucky, Lexington, Kentucky have also collaborated recently to develop mathematical models to study ingot stress crack formation and butt deformation[96], and to reduce aluminum ingot scrap. In Canada, University of British Columbia and Alcan International Ltd.

are also jointly pursuing modeling activities to generate hot tearing criteria for the D.C. casting process[5].

VI. SUMMARY AND CONCLUSIONS

Continuous casting processes for steel and aluminum alloys have different process design and operating parameters, owing to their differences in thermo-physical properties such as melting point, thermal conductivity, thermal contraction coefficient, and solidification shrinkage. However, the basis heat transfer processes characterizing the removal of superheat, latent heat and sensible heat are similar. Both the mold and water play significant roles in dictating the complex cooling phenomena under both transient and steady state conditions.

This paper shows how water-cooling governs the temperature of the metal strand, and how unsymmetrical or localized cooling problems can cause defects leading to high rejection rates and low productivity. Specific observations include:

(i) Empirical relations to describe cooling in the water channels are well established and used to optimize primary cooling in the mold during the continuous casting of steel. Hot face temperature controls interfacial heat transport at the meniscus, which greatly affects surface quality. Perhaps the optimization of mold water cooling and the related control of mold taper and mold distortion, which have been applied so successfully in the steel industry, could also help to improve the D.C. casting mold for aluminum.

(ii) In the case of continuous casting of steel, vapor film boiling dominates the heat extraction mechanism during spray cooling. As a result, the boiling water heat transfer coefficient is independent of strand surface temperature, and heat extraction is stably-controlled by water flow rate. In contrast, transition/nucleate boiling often arises during D.C. casting to cause aggressive cooling of the ingot surfaces. However, film boiling is desired during the transient cast start-up phase to reduce the effect of butt curl. Effects like water ejection and water incursion coupled with the rapidly changing ingot surface temperature during the transient phase can significantly complicate the heat transfer process. As a result, the process is extremely difficult to control.

(iii) Empirical relationships describing the variation of boiling water heat transfer coefficient with spray nozzle type, nozzle separation, distance of the nozzle from the surface of the strand and water flow rate have been established for secondary cooling of steel. However, the effects of surface finish and water quality/contamination have not been investigated. For D.C. casting of aluminum alloys, correlations for boiling water curves have been developed mainly under steady state conditions. Only a few studies for certain specific aluminum alloys are available, which can describe the boiling water heat transfer during the transient phase at which time the heat transfer coefficient can be a strong function of ingot surface temperature, water flow rate, distance from the impingement point, and the impingement point temperature.

(iv) Secondary cooling should be designed to cool the strand surface in a controlled, monotonic manner, in order to avoid severe temperature gradient fluctuations that cause cracks. Developments such as plateau cooling, air-mist cooling, and online process control with mathematical models has helped to improve secondary cooling in continuous casting of steel. A variety of processes have been developed for D.C. casting of aluminum.

(v) Despite decades of plant trials and increased process automation, quality problems related to water cooling such as butt curl and hot tear cracks still nag the D.C. casting industry. Different proprietary “recipes” are currently used by different aluminum companies to change casting variables as a function of time and alloy during start-up. There is recent recognition of the need for well-validated, fundamentally-based thermo-mechanical mathematical models of the D.C.

casting process to aid further improvements, including the optimization of water-cooling practices.

VII. ACKNOWLEDEMENTS

The authors wish to thank Natural Sciences and Engineering Research Council (NSERC), Canada for providing financial support for J. Sengupta and the Continuous Casting Consortium at the University of Illinois at Urbana-Champaign.

VIII. REFERENCES

1. C. Li and B.G. Thomas: Proceedings of the Brimacombe Memorial Symposium, Vancouver, Canada, Published by TMS, Warrendale, USA, pp. 17, 2000.
2. J. Sengupta, S. Cockcroft, D. Maijer, M. Wells, and A. Larouche: forthcoming in Metallurgical & Materials Transactions B.
3. J.F. Grandfield and P.T. McGlade: Materials Forum, **20**, pp. 29-51, 1996.
4. B.G. Thomas: in *The Encyclopedia of Materials: Science and Technology, Volume II*, Ed. D. Apelian, Elsevier Science Ltd., Oxford, UK,2000.
5. J. Sengupta: Ph. D., Department of Metals & Materials Engineering, University of British Columbia, Vancouver, Canada, 2002.
6. J.B. Wiskel: Ph. D., Department of Metals & Materials Engineering, University of British Columbia, Vancouver, Canada, 1996.
7. E.K. Jensen: Light Metals 1980, The Minerals, Metals and Materials Society, Warrendale, USA, pp. 631-642, 1980.
8. W.K.J. Jones, D. Xu, J.W. Evans, and D.P. Cook: Light Metals 1999, The Minerals, Metals & Materials Society, Warrendale, USA, pp. 841-845, 1999.
9. J.R. Davis: ed., ASM International, Materials Park, Ohio, USA1994.
10. P.W. Baker and P.T. McGlade: Light Metals 2001 (Ed. J. L. Anjier), The Minerals, Metals and Materials Society, Warrendale, USA, pp. 855-862, 2001.
11. X. Huang, B.G. Thomas, and F.M. Najjar: Metallurgical Transactions B, **23B**, pp. 339-356, 1992.
12. W. Droste and W. Schneider: Light Metals 1991 (Ed. E.L. Rooy), The Minerals, Metals & Materials Society, Warrendale, USA, pp. 945-951, 1991.
13. J. Sengupta, S. Cockcroft, D. Maijer, M. Wells, and A. Larouche: Journal of Light Metals, **2(3)**, pp. 137-148, 2002.
14. J.K. Brimacombe, I.V. Samarasekera, and J.E. Lait: in *Continuous Casting Vol. II: Heat Flow, Solidification and Crack Formation*, Ed. J.K. Brimacombe, I.V. Samarasekera, and J.E. Lait, The Iron and Steel Society of AIME, USA, pp. 1,1984.
15. S.C. Flood, P.A. Davidson, and S. Rogers: in *Modeling of Casting, Welding and Advanced Solidification Processes VII*, Ed. M.C.a.J. Campbell, The Minerals, Metals and Materials Society, Warrendale, USA, pp. 801,1995.
16. M. Zheng and L. Katgerman: in *Proceedings of the 22nd Riso International Symposium on Materials Science*, Ed. M.E. A.R. Dinesen, D. Juul Jensen, and S. Linderoth, Roskilde, Denmark, pp. 455-460,2001.
17. M. Trovant and S. Argyropoulos: Light Metals 1997 (Ed. R. Huglen), The Minerals, Metals and Materials Society, Warrendale, USA, pp. 927-931, 1997.
18. Y. Meng and B.G. Thomas: Metallurgical Transactions B, **34B**, pp. 707-725, 2003.
19. J. Birat, M. Larrecq, J. Lamant, and J. Petegnief: Mold Operation for Quality and Productivity (Edited by A.W. Cramb and E. Szekeres), ISS, Warrendale, USA, pp. 3-14, 1991.
20. M.A. Wells, D. Li, and S.L. Cockcroft: Metallurgical Transactions B, **32B**, pp. 929-939, 2000.
21. R.B. Mahapatra, J.K. Brimacombe, and I.V. Samarasekera: Metallurgical Transactions B, **22B**, pp. 875-888, 1991.
22. B.G. Thomas, D. Lui, and B. Ho: in *Sensors and Modeling in Materials Processing: Techniques and Applications*, 1997, Orlando, Florida, The Minerals, Metals and Materials Society, USA.
23. I.V. Samarasekera and J.K. Brimacombe: Canadian Metallurgical Quarterly, **18**, pp. 251-266, 1979.
24. Y. Meng and B.G. Thomas: Metallurgical Transactions B, **34B**, pp. 685-705, 2003.
25. H. Bai and B.G. Thomas: Metallurgical Transactions B, **32B**, pp. 269-284, 2001.
26. B.G. Thomas and S.P. Vanka: in *NSF Design, Service, Manufacturing and Industrial Innovation Research Conference, Puerto Rico*, 2002.

27. S. Engler, W. Schmitz, M.S. Ji, and A. Weiss: in *Proceedings of Symposium on Advances in Continuous Casting and Research Technology*, Ed. Abington Publishing, UK, pp. 192-204,1992.
28. G. Gruen, A. Buchholz, and D. Mortensen: Light Metals 2000 (Ed. R.D. Peterson), The Minerals, Metals and Materials Society, Warrendale, USA, pp. 573-578, 2000.
29. B.G. Thomas, A. Moitra, and R. McDavid: Iron and Steelmaker (USA), **23(4)**, pp. 57-70, 1996.
30. M.M. Wolf: BHM 2000, **145 (7)**, pp. 270-275, 2000.
31. R. Bommaraju, J.K. Brimacombe, and I.V. Samarasekera: ISS Transactions, **95-105**, 1984.
32. B.G. Thomas: Iron and Steelmaker (USA), (1-14), 1989.
33. B.G. Thomas: Metallurgical Transactions B, **33B**, pp. 795-812, 2002.
34. J.K. Brimacombe and K. Sorimachi: Metallurgical Transactions B, **8B**, pp. 489-505, 1977.
35. J.K. Brimacombe, F. Weinberg, and E.B. Hawbolt: Metallurgical Transactions B, **10B**, pp. 279-292, 1979.
36. J.M. Drezet, A. Bughardt, H.G. Fjaer, and B. Magnin: Materials Science Forum 2000, **329-330**, pp. 493-500, 2000.
37. W. Schneider and W. Reif: in *Proceedings of Symposium on Advances in Continuous Casting and Research Technology*, 1992, Cairo, Egypt, Abington Publishing, UK.
38. D.C. Weckman and P. Niessen: Metallurgical Transactions B, **13B**, pp. 593-602, 1982.
39. K. Ho and R.D. Pehlke: Metallurgical Transactions B, **16B**, pp. 585-594, 1985.
40. Y. Nishida, W. Droste, and E. Engler: Metallurgical Transactions B, **17B**, pp. 833-844, 1986.
41. A.A. Nofal: in *Proceedings of Symposium on Advances in Continuous Casting and Research Technology*, 1992, Cairo, Egypt, Abington Publishing, UK.
42. R. Mitamura, T. Ito, Y. Takahashi, and T. Hiraoka: Light Metals 1998 (Ed. R. Huglen), The Minerals, Metals and Materials Society, Warrendale, USA, pp. 281-291, 1978.
43. J.-M. Drezet: Ph. D., Department of Materials, Ecole Polytechnique Federale de Lausanne, Lausanne, Switzerland, 1996.
44. R.A. Hardin, K. Liu, A. Kapoor, and C. Beckermann: Metallurgical Transactions B, **34B**, pp. 297-306, 2003.
45. L. Yu: Ph.D., Department of Mechanical and Industrial Engineering, University of Illinois, Urbana-Champaign, USA, 1996.
46. H.M. Tansi and G.E. Totten: in *Proceedings of the 3rd International Conference on Quenching and Control of Distortion*, 1999, Prague, Czech Republic.
47. J.K. Brimacombe, P.K. Agarwal, S. Hibbins, B. Prabhakar, and L.A. Baptista: in *Continuous Casting Vol. II: Heat Flow, Solidification and Crack Formation*, Ed. J.K. Brimacombe, I.V. Samarasekera, and J.E. Lait, The Iron and Steel Society of AIME, USA, pp. 109-123,1984.
48. F.M. White: *Heat and Mass Transfer*, A-W Publishing Company,1991.
49. A. Larouche, Y. Caron, and D. Kocaefe: Light Metals 1998 (Ed. B. Welch), The Minerals, Metals and Materials Society, Warrendale, USA, pp. 1059-1064, 1998.
50. G.P. Grealy, J.L. Davis, E.K. Jensen, P.A. Tondel, and J. Moritz: Light Metals 2001 (Ed. J. L. Anjier), The Minerals, Metals & Materials Society, Warrendale, USA, pp. 813-821, 2001.
51. W. Droste, J.-M. Drezet, G.-U. Grun, and W. Schneider: Continuous Casting (Ed. K. Ehrke and W. Schneider), Wiley-VCH, pp. 177-183, 2000.
52. J. Sengupta, D. Maijer, M.A. Wells, S.L. Cockcroft, and A. Larouche: Light Metals 2001 (Ed. J. L. Anjier), The Minerals, Metals and Materials Society, Warrendale, USA, pp. 879-885, 2001.
53. B.G. Thomas, J.K. Brimacombe, and I.V. Samarasekera: Transactions of the Iron and Steel Society, **7**, pp. 7-20, 1986.
54. J. Du, B.S.-J. Kang, K.-M. Chang, and J. Harris: Light Metals 1998 (Ed. B. Welch), The Minerals, Metals & Materials Society, Warrendale, USA, pp. 1025-1029, 1998.
55. L.J. Colley: M.A.Sc., Department of Metals and Materials Engineering, University of British Columbia, Vancouver, Canada, 2003.
56. J.K. Brimacombe: in *Continous Casting Vol. II: Heat Flow, Solidification and Crack Formation*, Ed. J.K. Brimacombe, I.V. Samarasekera, and J.E. Lait, Iron and Steel Society of AIME, USA, pp. 199-214,1984.
57. J.E. Jacoby: in *5th Australasian Asian Pacific Conference on Aluminum Cast House Technology*, 1997, The Minerals, Metals and Materials Society.
58. J.B. Wiskel and S.L. Cockcroft: Metallurgical Transactions B, **27B**, pp. 129-137, 1996.
59. C.A. Sleicher and M.W. Rousse: International Journal of Heat and Mass Transfer, **18(5)**, pp. 677-683, 1975.
60. F.W. Dittus and L.M.K. Boelter: University of California Publications in Engineering, (2), pp. 443-461, 1930.
61. M. Mitsutsuka: Tetsu-to-Hagane, **54**, pp. 1457-1471, 1968.
62. M. Shimada and M. Mitsutsuka: Tetsu-to-Hagane, **52**, pp. 1643, 1966.
63. E. Mizikar: Iron Steel Engineer, **47**, pp. 53-60, 1970.

64. R. Alberny, Ed. Committee of European Communities, Luxembourg, IPC Science and Technology Press, pp. 278-335,1977.
65. T. Nozaki, J. Matsuno, K. Murata, H. Ooi, and M. Kodama: Trans ISIJ, **18**, pp. 330-338, 1978.
66. E. Bolle and J.C. Moureau: in *Int. Conf. on Heat and Mass Transfer Metallurgical Processes*, 1979, Yugoslavia.
67. H. Kraushaar, R. Jeschar, V. Heidt, E.K. Jensen, and W. Schneider: Light Metals 1995 (Ed. J. Evans), The Minerals, Metals and Materials Society, Warrendale, USA, pp. 1055-1059, 1995.
68. J. Langlais, T. Bourgeois, Y. Caron, G. Beland, and D. Bernard: Light Metals 1995 (Ed. J. Evans), The Minerals, Metals and Materials Society, Warrendale, USA, pp. 979-986, 1995.
69. L. Maenner, B. Magnin, and Y. Caratini: Light Metals 1997 (Ed. R. Huglen), The Minerals, Metals and Materials Society, Warrendale, USA, pp. 701-707, 1997.
70. A. Larouche, J. Langlais, T. Bourgeois, and A. Gendron: Light Metals 1999 (Ed. M. Bouchard and A. Faucher), MetSoc, Warrendale, USA, pp. 235-245, 1999.
71. I.J. Opstelten and J. M.Rabenberg: Light Metals 1999 (Ed. C. E. Eckert), The Minerals, Metals and Materials Society, Warrendale, USA, pp. 729-735, 1999.
72. J.Z. Jr., L. Katgerman, I.J. Opstelten, and J.M. Rabenberg: Light Metals 2001 (Ed. J. L. Anjier), The Minerals, Metals and Materials Society, Warrendale, USA, pp. 873-878, 2001.
73. D. Li, M.A. Wells, and G. Lockhart: Light Metals 2001 (Ed. J. L. Anjier), The Minerals, Metals and Materials Society, Warrendale, USA, pp. 865-871, 2001.
74. L.I. Kiss, T. Meenken, A. Charette, Y. Lefebvre, and R. Levesque: Light Metals 2002 (Ed. W. Schneider), The Minerals, Metals and Materials Society, pp. 981-985, 2002.
75. S.G. Hibbins: in *Continuous Casting Vol. II: Heat Flow, Solidification and Crack Formation*, Ed. J.K. Brimacombe, I.V. Samarasekera, and J.E. Lait, The Iron and Steel Society of AIME, USA, pp. 139-151,1984.
76. J.B. Wiskel and S.L. Cockcroft: Metallurgical Transactions B, **27B**, pp. 119-127, 1996.
77. J.A. Bakken and T. Bergstrom: Light Metals 1986, The Minerals, Metals and Materials Society, Warrendale, USA, pp. 883-889, 1986.
78. E.K. Jensen, S. Johansen, T. Bergstrom, and J.A. Bakken: Light Metals 1986, The Minerals, Metals and Materials Society, Warrendale, USA, pp. 891-896, 1986.
79. Y. Watanabe and N. Hayashi: Light Metals 1996 (Ed. W. Hale), The Minerals, Metals and Materials Society, Warrendale, USA, pp. 979-984, 1996.
80. J. Sengupta, D. Maijer, M. A. Wells, S.L. Cockcroft, and A. Larouche: Light Metals 2003 (Ed. W. Schneider), The Minerals, Metals & Materials Society, Warrendale, USA, pp. 841-847, 2003.
81. L. Bendig, M. Raudensky, and J. Horsky: in *SteelMaking Conference Proceedings*, 1995.
82. M. El-Bealy, N. Leskinen, and H. Fredriksson: Ironmaking and Steelmaking, **22(3)**, pp. 246-255, 1995.
83. L.K. Chiang: in *57th Electric Furnace Conference*, 1999, Pittsburgh, USA, Iron & Steel Society, Warrendale, USA.
84. S.-M. Lee and S.-Y. Jang: ISIJ International (Japan), **36**(Supplementary on Science and Technology of Steelmaking), pp. 208-210, 1996.
85. T. Kohno, T. Shima, T. Kuwabara, T. Yamamoto, M. Wake, and T. Tsuneoka: in *Continuous Casting Vol. II: Heat Flow, Solidification and Crack Formation*, Ed. I.V.S. J.K. Brimacombe, and J.E. Lait, The Iron and Steel Society of AIME, USA, pp. 133-137,1984.
86. L.A. Baptista: M.A.Sc., Department of Metals & Materials Engineering, University of British Columbia, Vancouver, Canada, 1979.
87. Y. Caron and A. Larouche: Light Metals 1996 (Ed. W. Hale), The Minerals, Metals & Materials Society, Warrendale, USA., pp. 963-969, 1996.
88. W. Schneider and E.K. Jensen: Light Metals 1990 (Ed. C. M. Bickert), The Minerals, Metals and Materials Society, Warrendale, USA, pp. 931-936, 1990.
89. W. Schneider: Light Metals 2002 (Ed. W. Schneider), The Minerals, Metals & Materials Society, Warrendale, USA., pp. 953-960, 2002.
90. H. Yu: Light Metals 1980, The Minerals, Metals & Materials Society, Warrendale, USA, pp. 613-628, 1980.
91. I. Wagstaff, U.S. Patent # 4,693,298, 1987.
92. N.B. Bryson, U.S. Patent # 3,411,079, Casting of Aluminum Ingots, 1969.
93. A. Moitra: Ph.D., Mechanical & Industrial Engineering, University of Illinois, Urbana-Champaign, USA, 1993.
94. Trademark of MARC Analysis Research Corporation, Palo Alto, USA.
95. VIR[CAST] News, Newsletter edited by Calcom, Switzerland, 1st edition (Spring), 2002.
96. Aluminum: Project Fact Sheet, Newsletter published by Office of Industrial Technologies, Energy Efficiency, and Renewable Energy, U. S. Department of Energy (DoE), Washington, D.C., 2000.

LIST OF SYMBOLS

Symbol	Description	Unit
	LATIN SYMBOLS	
A	Fitting parameter	---
b	Heat input coefficient	$Jm^{-2}K^{-1}s^{-0.5}$
Bi	Biot number	---
c	Fitting parameter	---
c_1, c_2	Empirical constants	---
cp	Specific heat	$Jkg^{-1}K^{-1}$
h	Convective heat transfer coefficient	$Wm^{-2}K^{-1}$
h_{spray}	Spray water heat transfer coefficient	$Wm^{-2}K^{-1}$
h_w	Convective heat transfer coefficient between mold and cooling water	$Wm^{-2}K^{-1}$
k	Thermal conductivity	$Wm^{-1}K^{-1}$
k_{water}	Thermal conductivity of water	$Wm^{-1}K^{-1}$
Pe	Peclet number	---
Pr_{waterw}	Prandtl number of water at the mold cold face temperature	---
R	Size of casting	m
Re_{waterf}	Reynolds number at average of mold cold face and cooling water temperatures	---
V	Casting speed	ms^{-1}
$\dot{W}$	Water flow rate	$lm^{-2}s^{-1}$
	GREEK SYMBOLS	
ρ	Density	kgm^{-3}

LIST OF FIGURES

Figure 1 – Schematic of (a) the continuous casting process for steel slabs and billets[4], and (b) the D.C. casting process for aluminum sheet ingots[5,6].

Figure 2 – Schematic of cooling processes, for (a) continuous casting of steel[14] and (b) D.C. casting of aluminum[5].

Figure 3 – Primary cooling during continuous casting (a) temperature profile across the mold and shell (steel), and thermal resistances[17,18], and (b) schematic of zones (aluminum)[22].

Figure 4 – Strand surface morphologies for typical (a) continuous cast steel and (b) D.C. cast aluminum alloys[20].

Figure 5 – Schematic of phenomena related to heat transfer inside and below the mold during continuous casting of steel[24].

Figure 6 – Flow pattern (left side) and velocities (right side) generated with different metal entry systems during D.C. casting: (a) vertical entry, (b) horizontal entry, (c) oblique entry, and (d) entry through a distribution bag[27].

Figure 7 – Effect of high (a) and low (b) meniscus level on UCD and temperature contours in the mold region of D.C. casting[41].

Figure 8 – (a) Secondary cooling during continuous casting of steel (a) typical arrangement of spray nozzles and support rolls[44], (b) schematic of zones[24], and (c) detail of water spray cooling process[46].

Figure 9 – (a) Secondary cooling regimes during D.C. casting of aluminum[20], and (b) detail of water film cooling process[46].

Figure 10 – Generic boiling curve for water-cooling indicating the different heat transfer regimes[48].

Figure 11 – Different boiling phenomena observed on D.C. cast ingot rolling surface during start-up showing evolution of semi-elliptical-steam barrier region of film boiling in hotter bottom-center region of ingot surface, which collapses with time (after References 49 and 50).

Figure 12 – Cooling and deformation of ingot base during the start-up of D.C. casting, showing high contact near the centre of the ingot (Region A), and entry of secondary cooling water near outer edges (Region B)[5].

Figure 13 – Typical surface temperature profile and cooling regimes along strand length during continuous casting of (a) steel[24] and (b) aluminum[5].

Figure 14 – Schematic of crack defects in continuous casting of steel[53].

Figure 15 – Schematic of crack defects related to secondary cooling during D.C. casting of aluminum[54].

Figure 16 – Typical boiling curves and operating temperature ranges in the secondary cooling regime for continuous casting of steel[47] and D.C. casting of aluminum[20].

Figure 17 - Effect of initial sample temperature on calculated boiling curves[20] (as-cast AA5182, water flow rate = 0.38 ls^{-1}) for: (a) the impingement zone, and (b) the streaming zone.

Figure 18 – Distribution of total heat removed from the shell at different locations during the continuous casting of steel[24].

Figure 19 - Temperature profiles and shell thickness predicted in cross-sections through the strand taken at mold exit and during secondary cooling for continuous casting of steel[45].

Figure 20 –Temperature profiles and shell thickness predicted in cross-sections through the ingot during secondary cooling taken ~375s after startup for D.C. casting of aluminum[2].

Figure 21 – Surface temperature contours on the narrow and rolling faces of a D.C. cast aluminum ingot at ~375s after start-up[2,5,80].

Figure 22 - Design and process parameters important to heat transfer during start-up of D.C. casting[87].

TABLES

Table 1 – Thermophysical properties of steel and aluminum[9-11].

Thermophysical Properties	Liquid Steel	Liquid Aluminum	Solid Steel	Solid Aluminum
Liquidus Temperature (°C)	1525	650	---	---
Density (kgm^{-3})	7020	2400	8000	2600
Specific Heat ($J/kg^{-1}K^{-1}$)	680	1300	690	900
Thermal Conductivity ($Wm^{-1}K^{-1}$)	26	90	29	190
Thermal diffusivity (m^2s^{-1})	0.54×10^{-5}	2.9×10^{-5}	0.53×10^{-5}	8.1×10^{-5}
Latent heat of fusion (Jm^{-3})	---	---	21.8×10^{8}	9.4×10^{8}
Solidification shrinkage (%)	---	---	2.5	6.5
Thermal contraction coefficient (K^{-1})	---	---	12×10^{-6}	24×10^{-6}

FIGURES

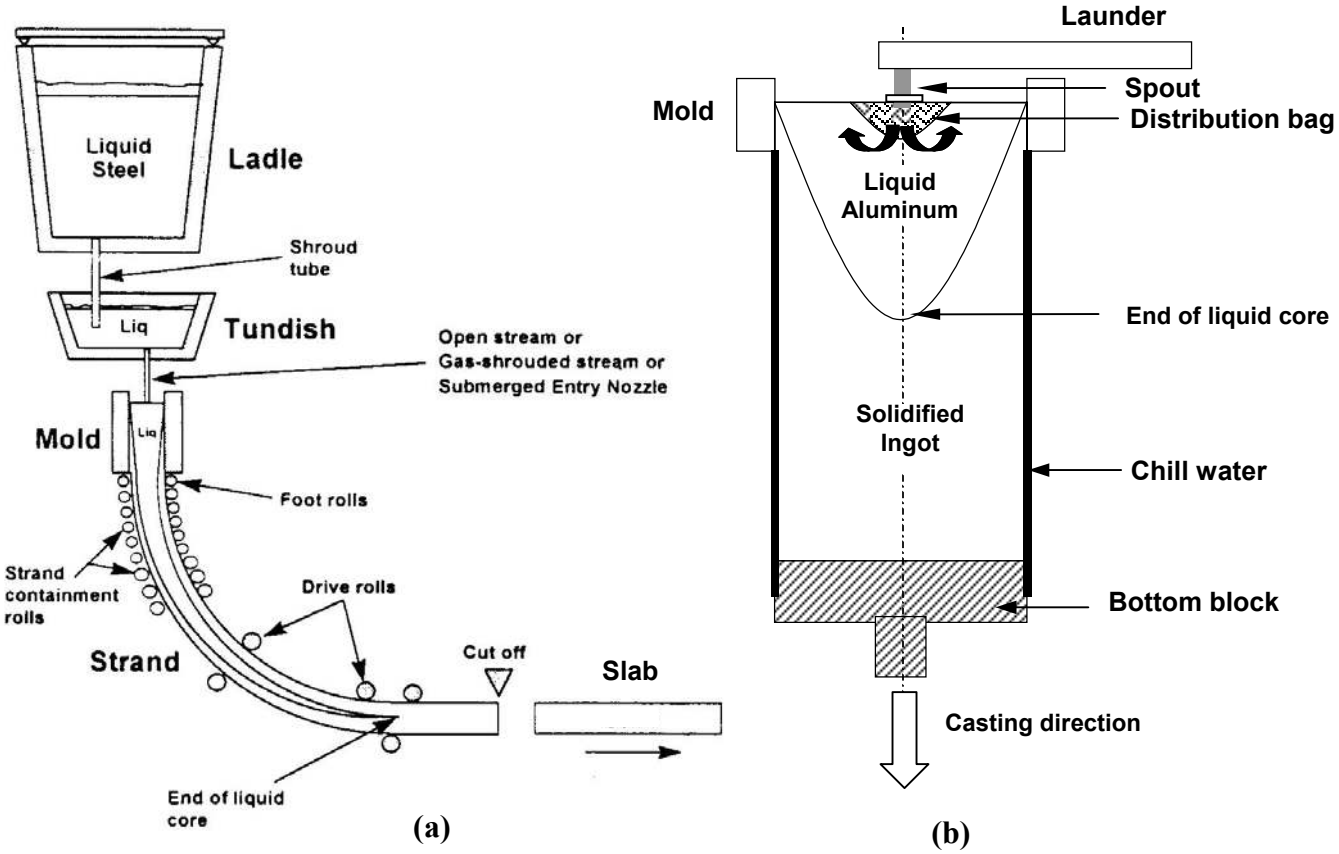

Figure 1 – Schematic of (a) the continuous casting process for steel slabs and billets[4], and (b) the D.C. casting process for aluminum sheet ingots[5,6].

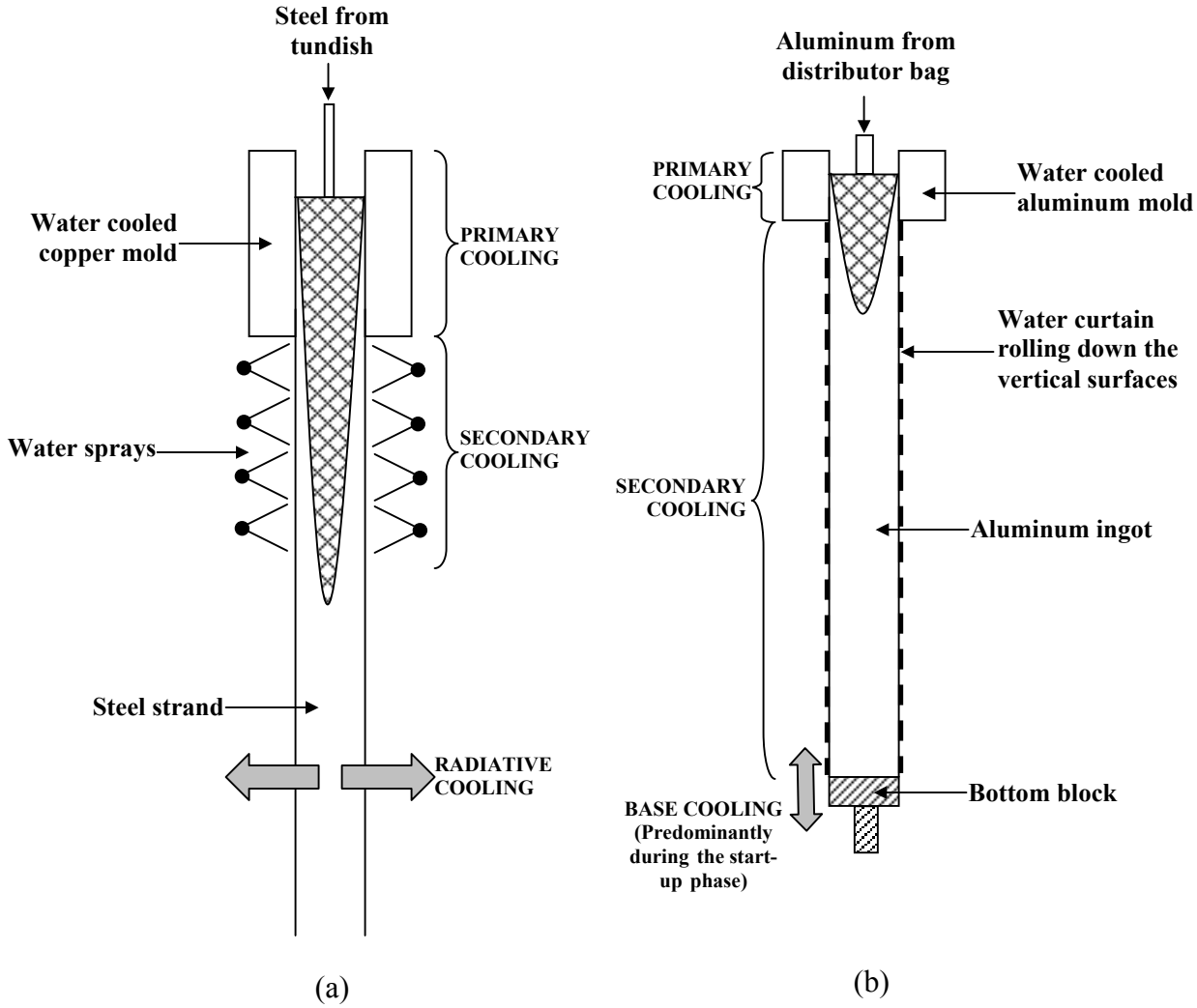

Figure 2 – Schematic of cooling processes, for (a) continuous casting of steel[14] and (b) D.C. casting of aluminum[5].

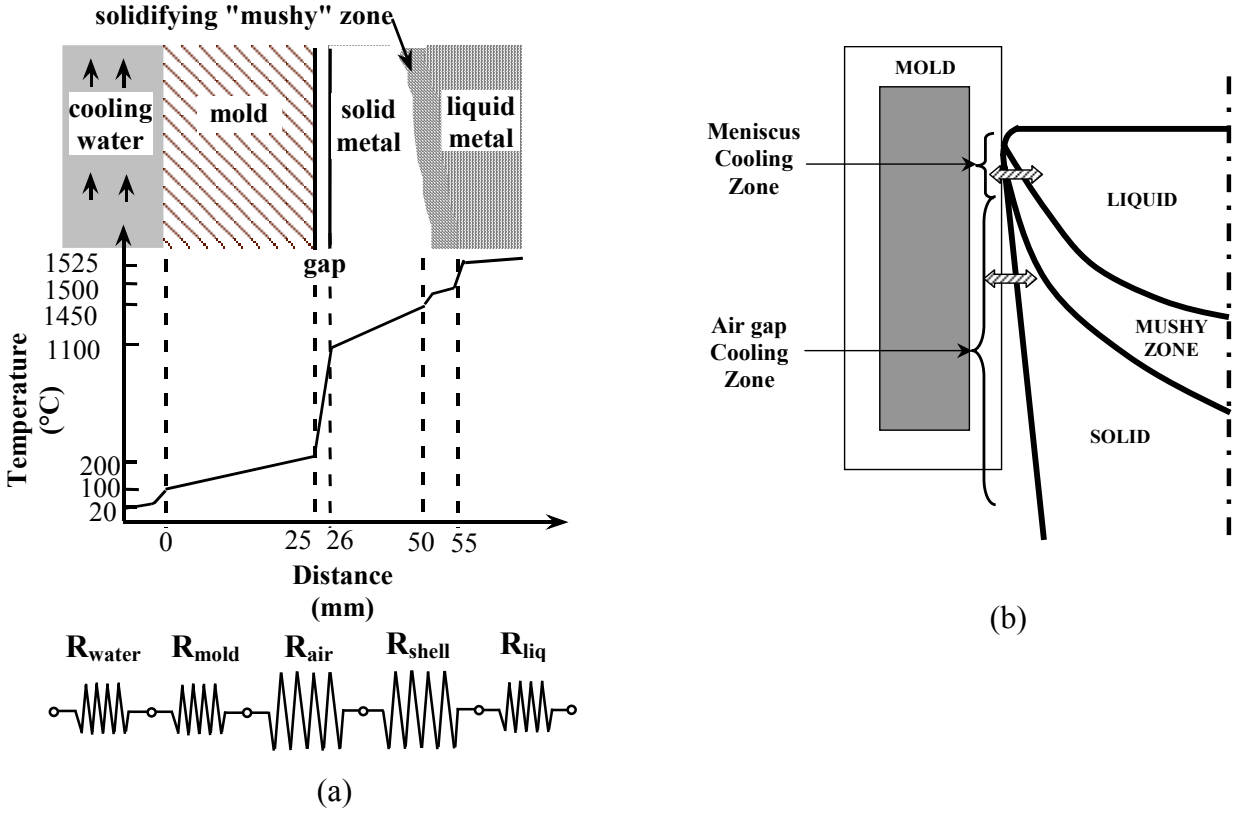

Figure 3 – Primary cooling during continuous casting (a) temperature profile across the mold and shell (steel), and thermal resistances[17,18], and (b) schematic of zones (aluminum)[22].

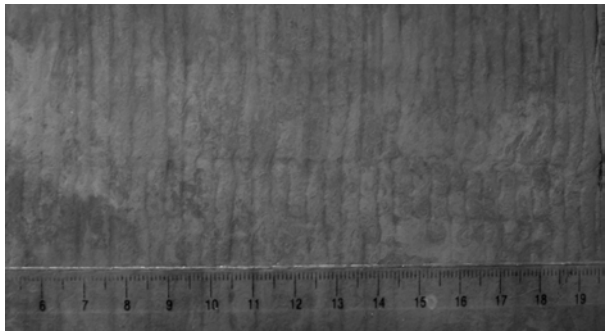

Low Carbon (Fe-0.05%C)

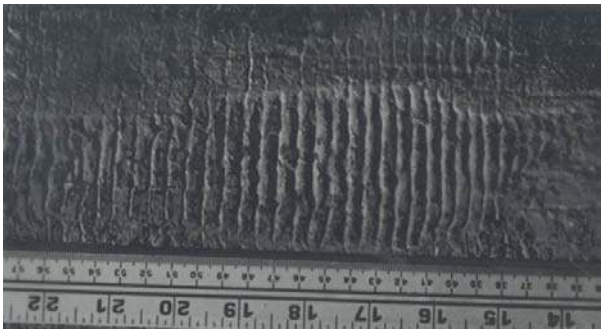

Peritectic (Fe-0.1%C)

(a)

AA1050 (Al >99.5%)

AA3004 (Al-1%Mn-1%Mg)

AA5182 (Al-4.5%Mg)

(b)

Figure 4 – Strand surface morphologies for typical (a) continuous cast steel and (b) D.C. cast aluminum alloys[20] (Casting direction is to the right).

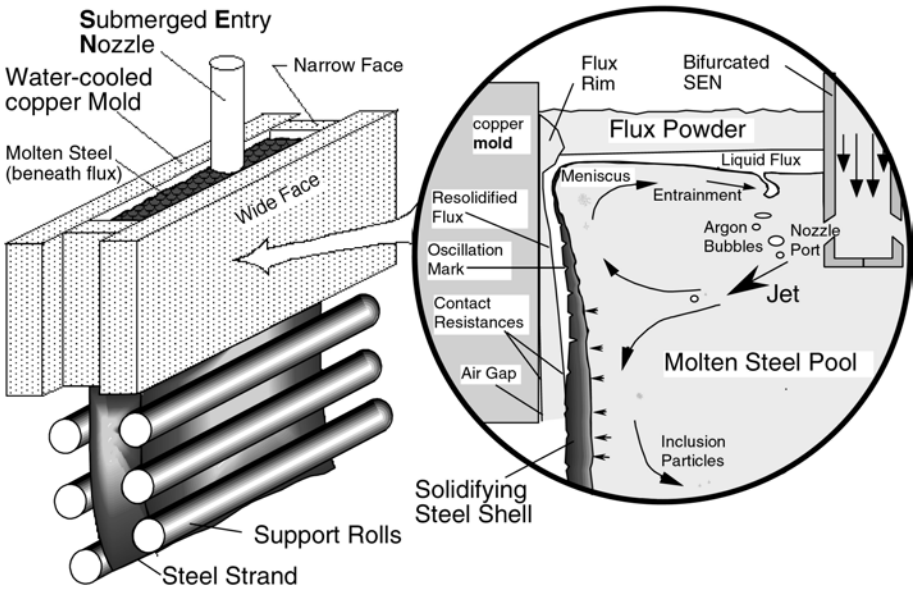

Figure 5 – Schematic of phenomena related to heat transfer inside and below the mold during continuous casting of steel[24].

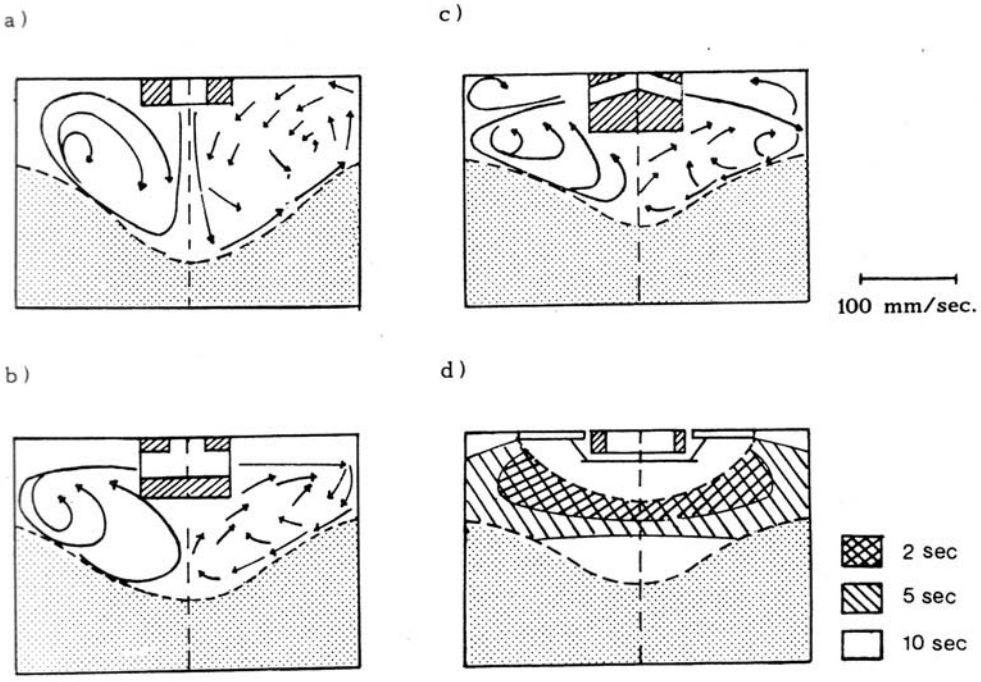

Figure 6 – Flow pattern (left side) and velocities (right side) and dye residence times (lower right) generated with different metal entry systems during D.C. casting: (a) vertical entry, (b) horizontal entry, (c) oblique entry, and (d) entry through a distribution bag[27].

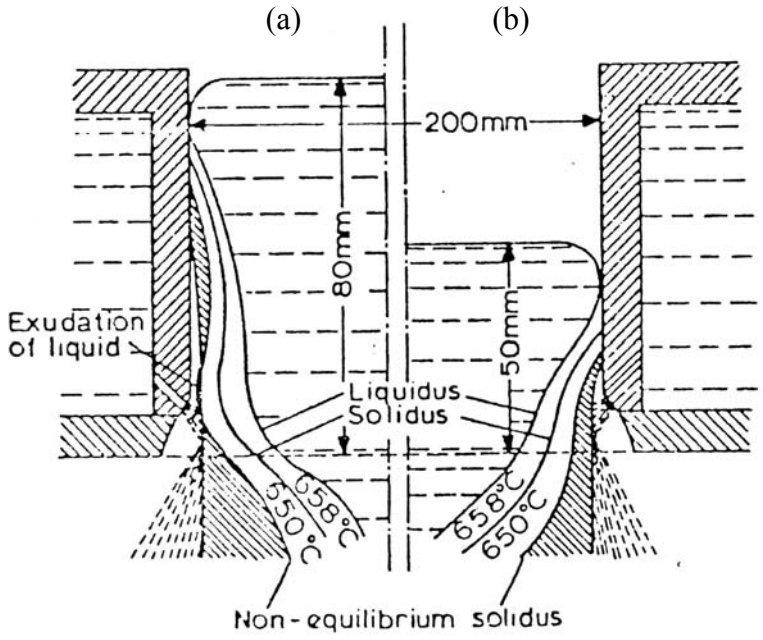

Figure 7 – Effect of high (a) and low (b) meniscus level on UCD and temperature contours in the mold region of D.C. casting[41].

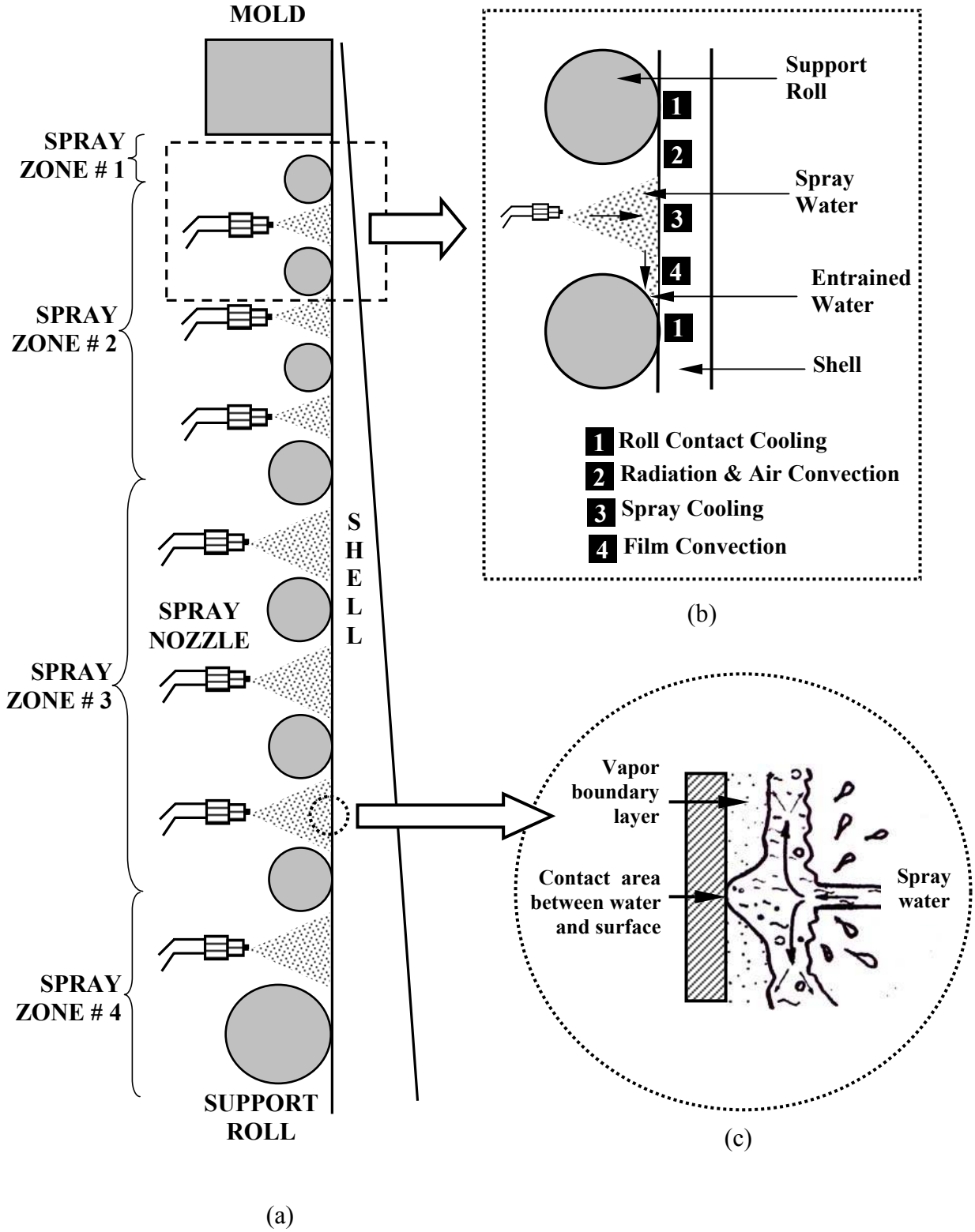

Figure 8 – (a) Secondary cooling during continuous casting of steel (a) typical arrangement of spray nozzles and support rolls[44], (b) schematic of zones[24], and (c) detail of water spray cooling process[46].

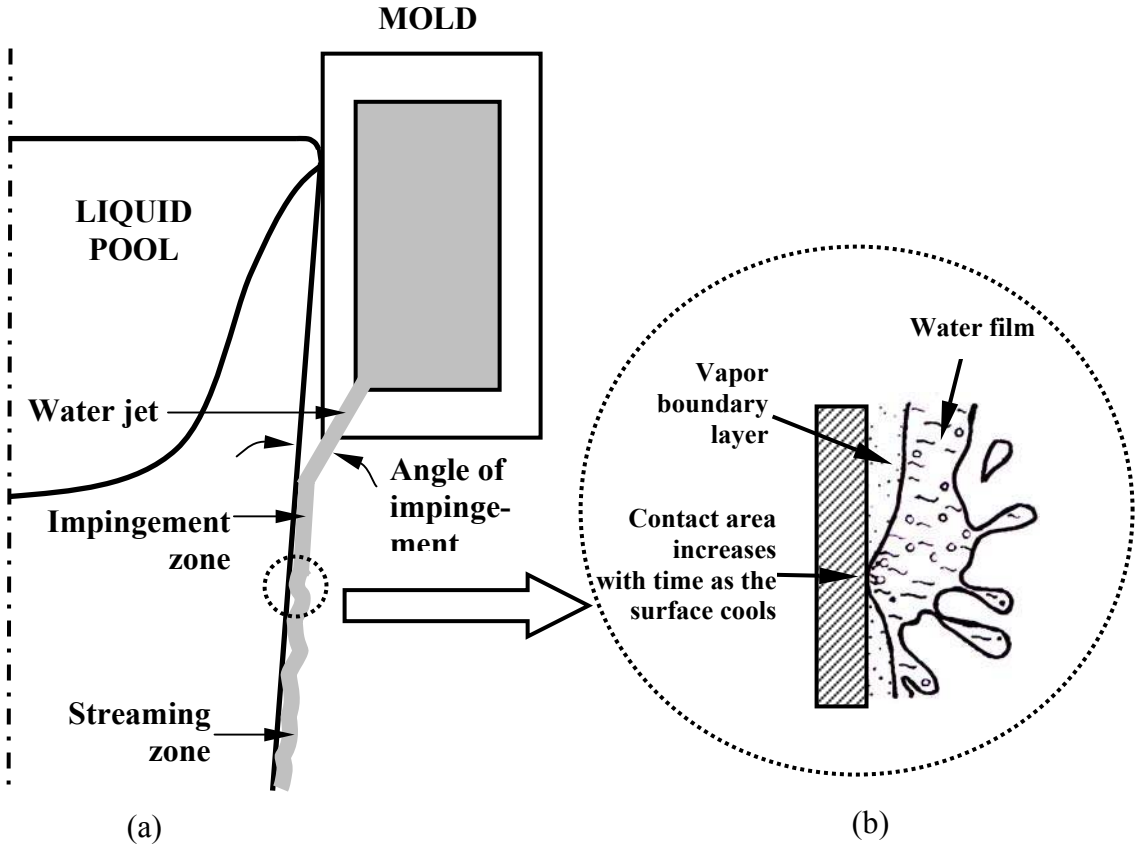

Figure 9 – (a) Secondary cooling regimes during D.C. casting of aluminum[20], and (b) detail of water film cooling process[46].

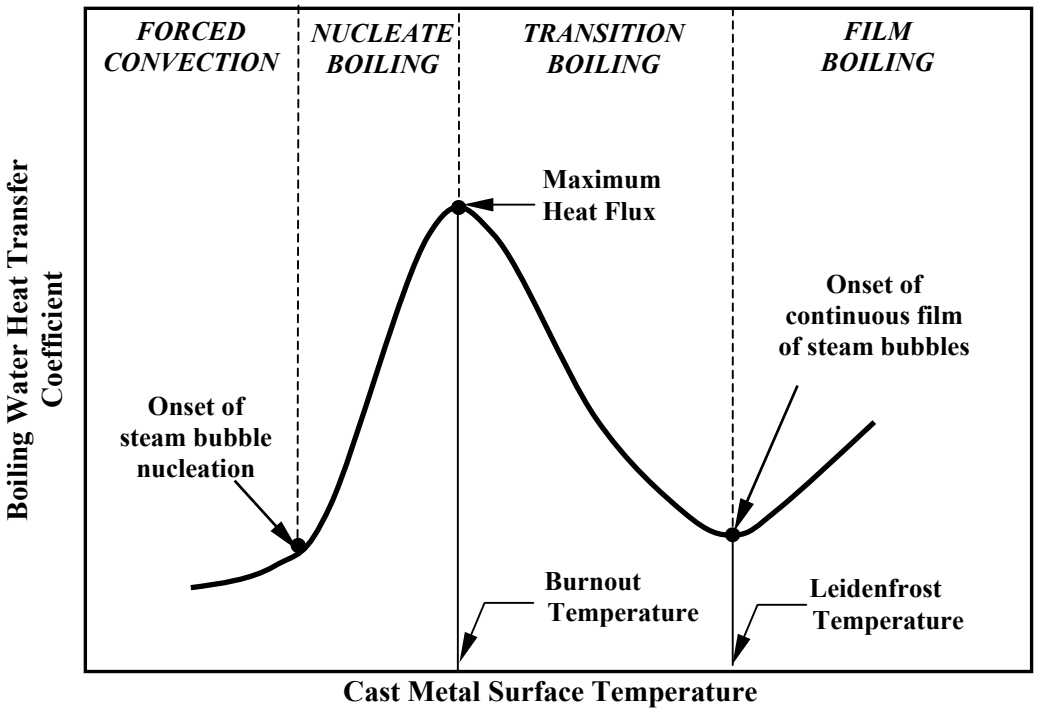

Figure 10 – Generic boiling curve for water-cooling indicating the different heat transfer regimes[48].

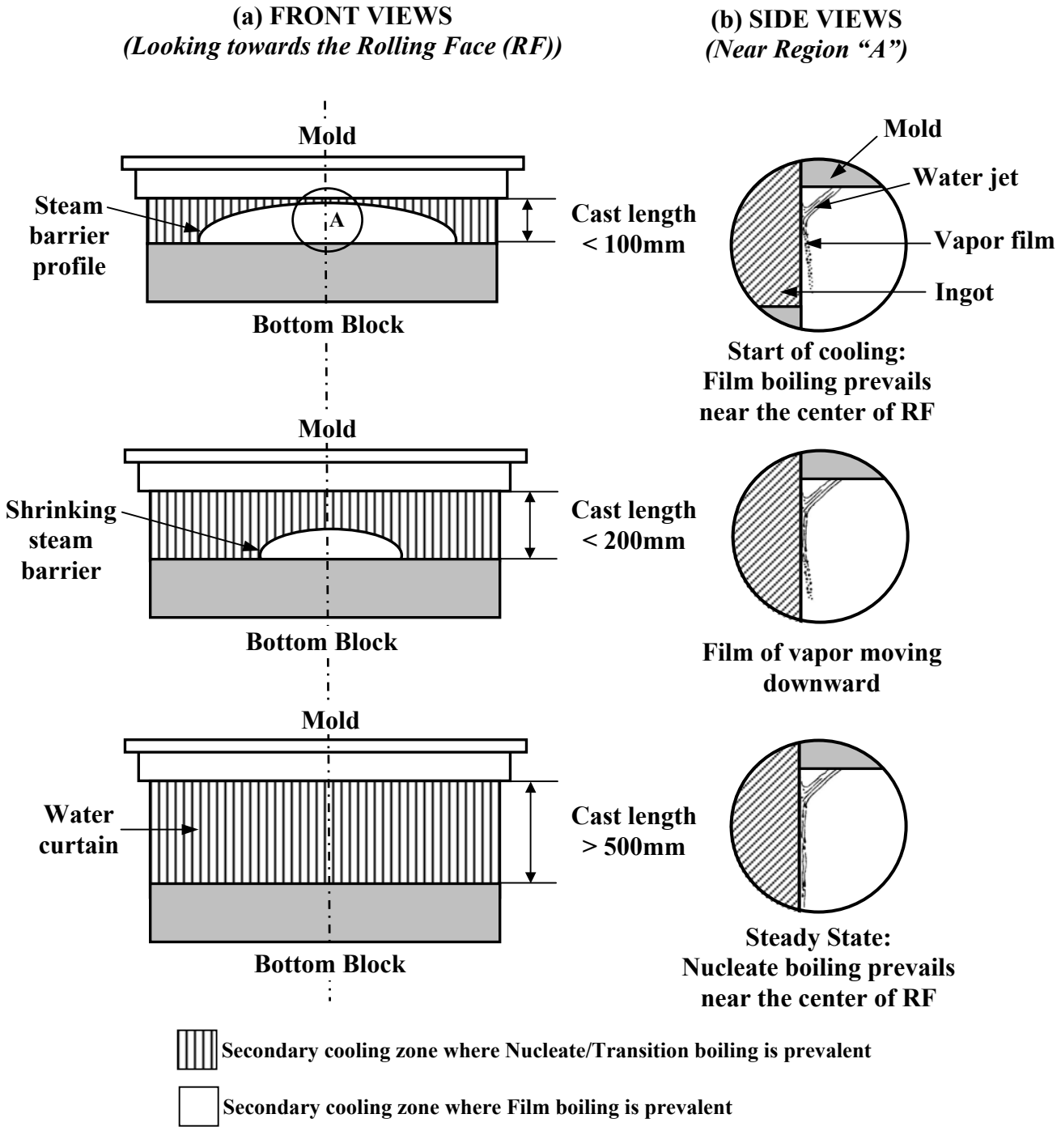

Figure 11 – Different boiling phenomena observed on D.C. cast ingot rolling surface during start-up showing evolution of semi-elliptical-steam barrier region of film boiling in hotter bottom-center region of ingot surface, which collapses with time (after References 49 and 50).

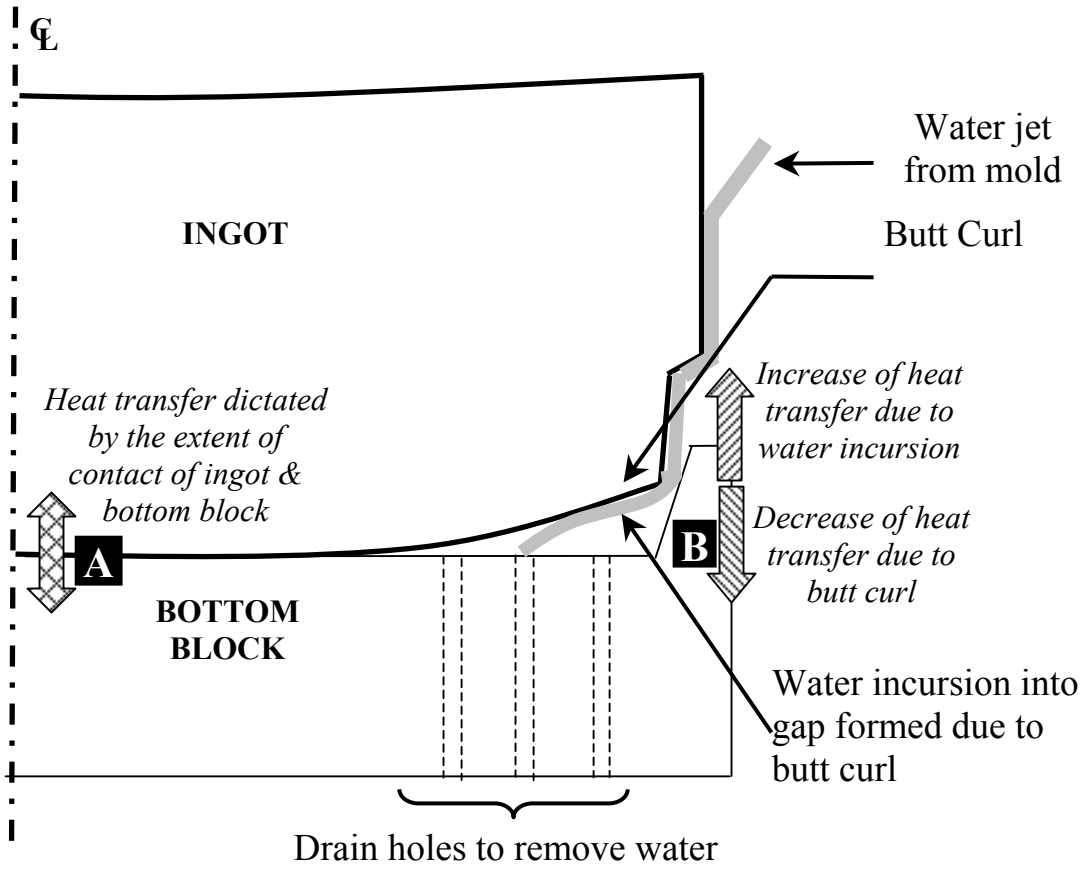

Figure 12 – Cooling and deformation of ingot base during the start-up of D.C. casting, showing high contact near the centre of the ingot (Region A), and entry of secondary cooling water near outer edges (Region B)[5].

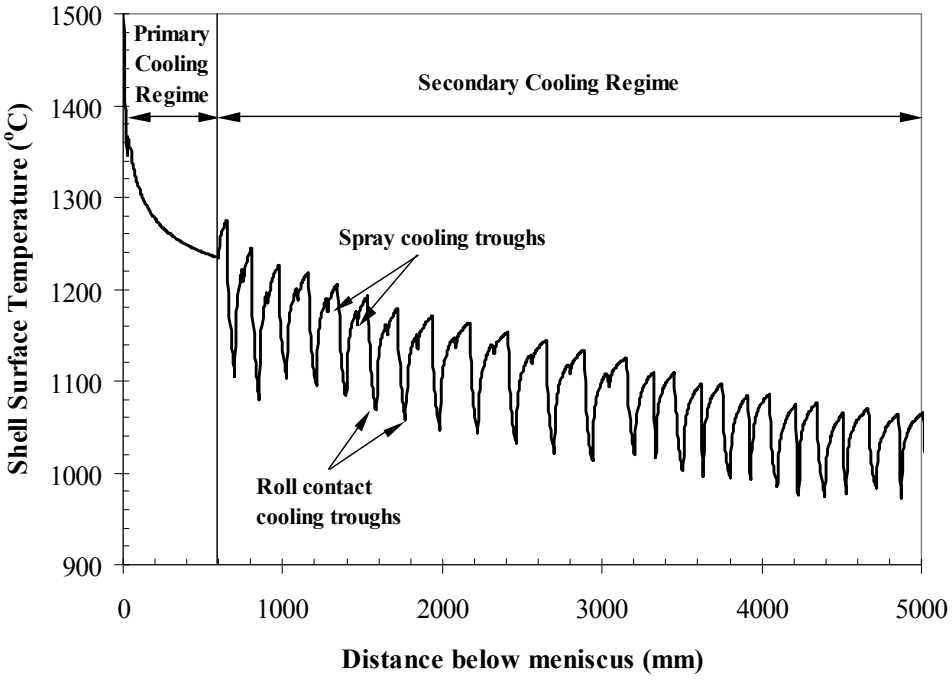

(a)

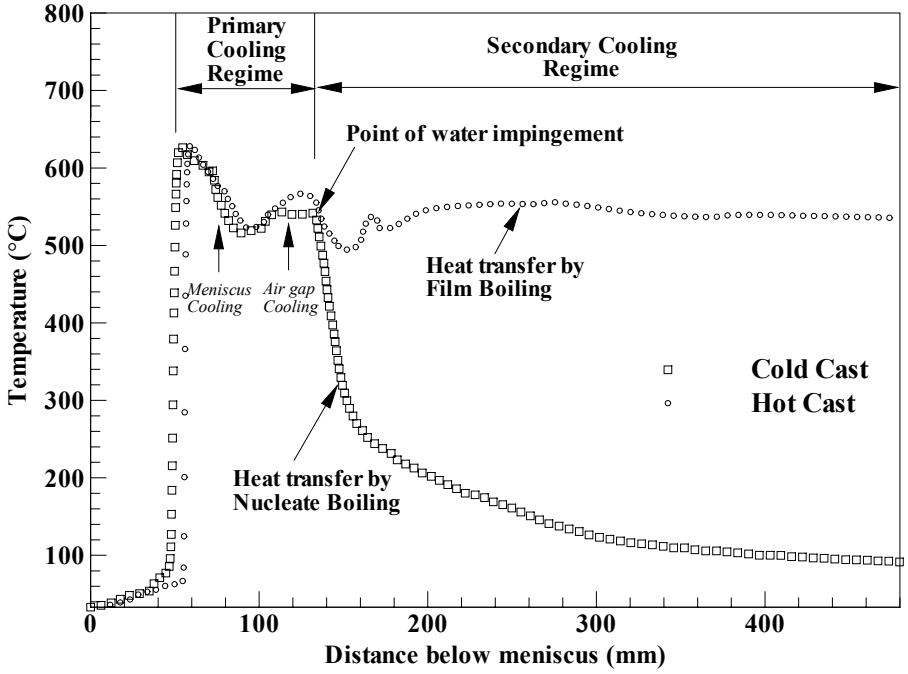

(b)

Figure 13 – Typical surface temperature profile and cooling regimes along strand length during continuous casting of (a) steel[24] and (b) aluminum[5].

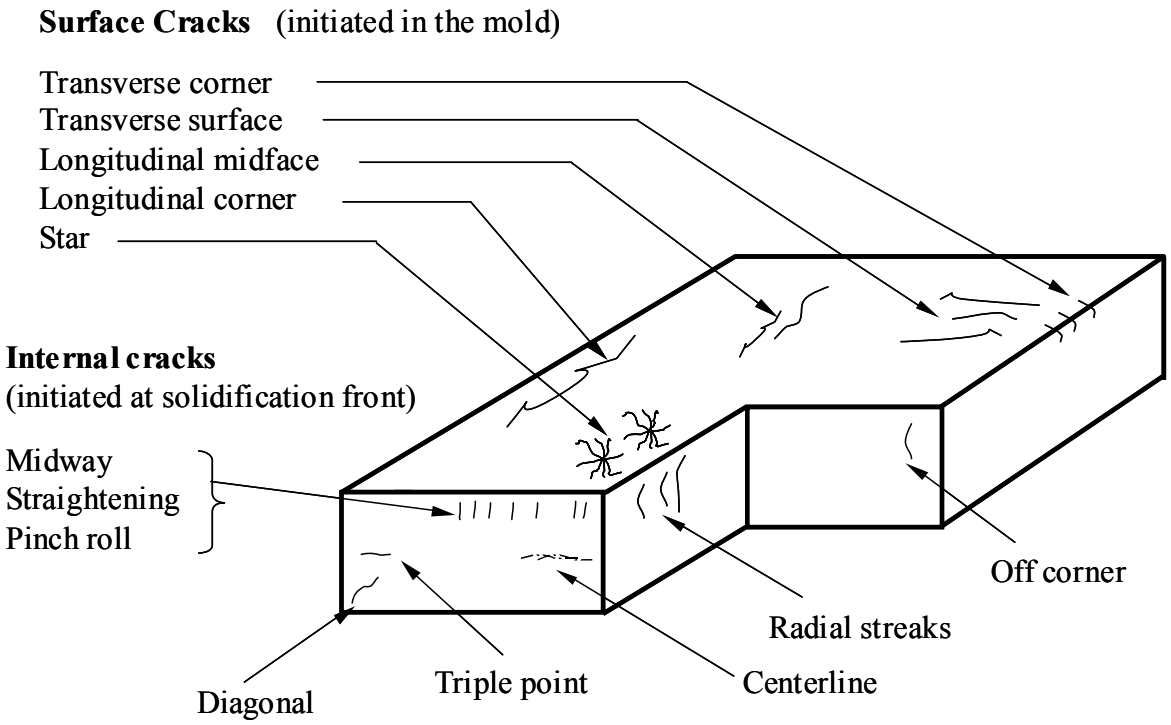

Figure 14 – Schematic of crack defects in continuous casting of steel[53].

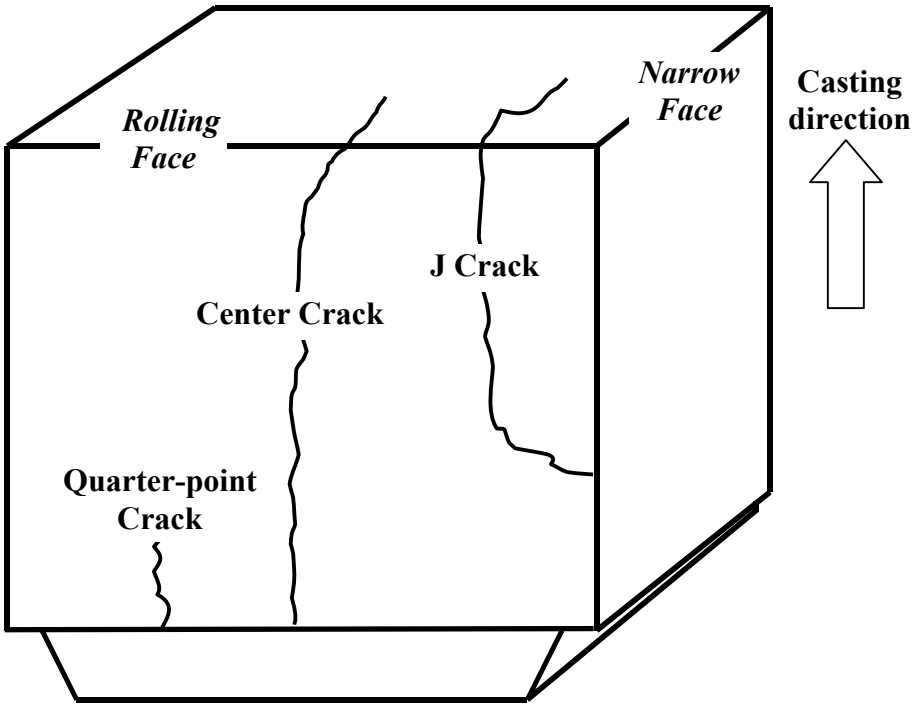

Figure 15 – Schematic of crack defects related to secondary cooling during D.C. casting of aluminum[54].

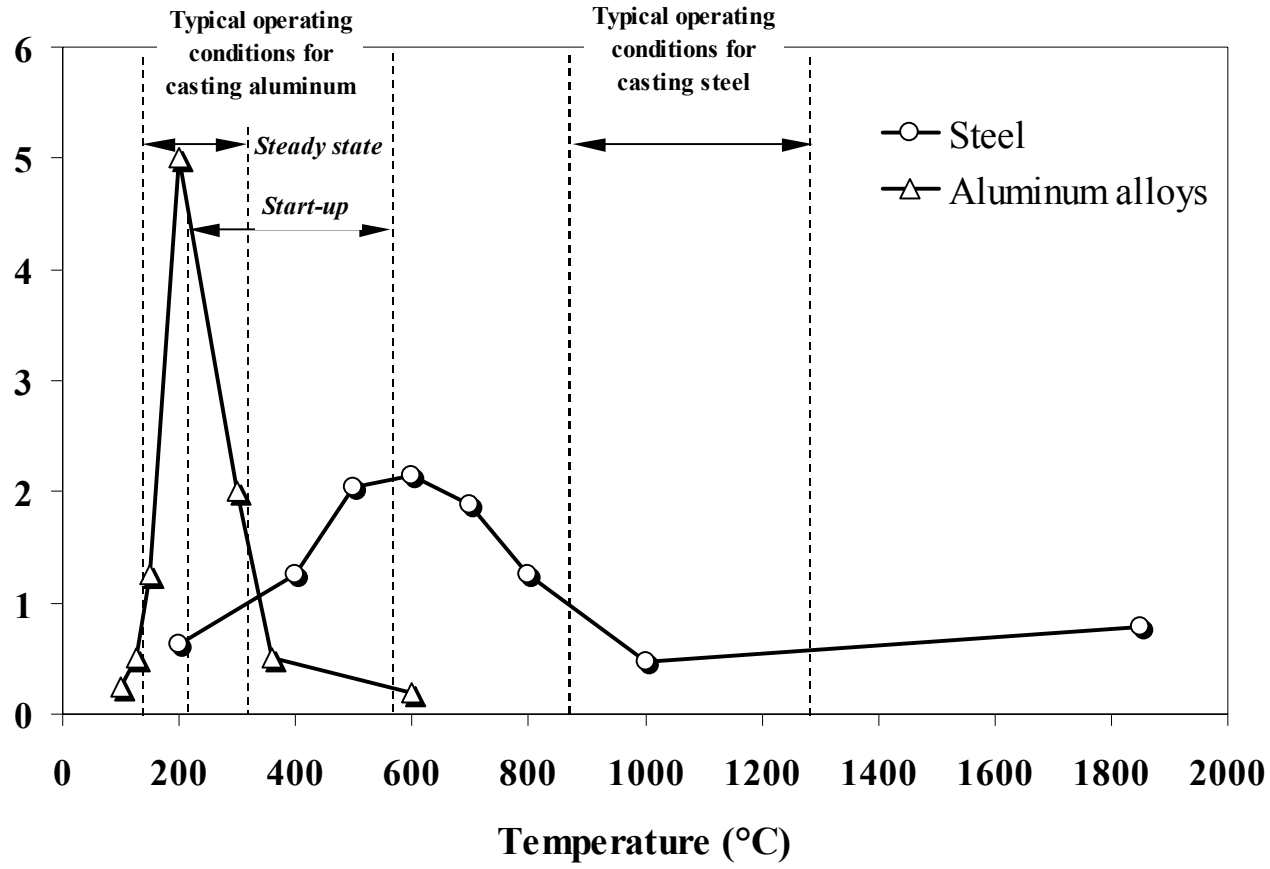

Figure 16 – Typical boiling curves and operating temperature ranges in the secondary cooling regime for continuous casting of steel[47] and D.C. casting of aluminum[20].

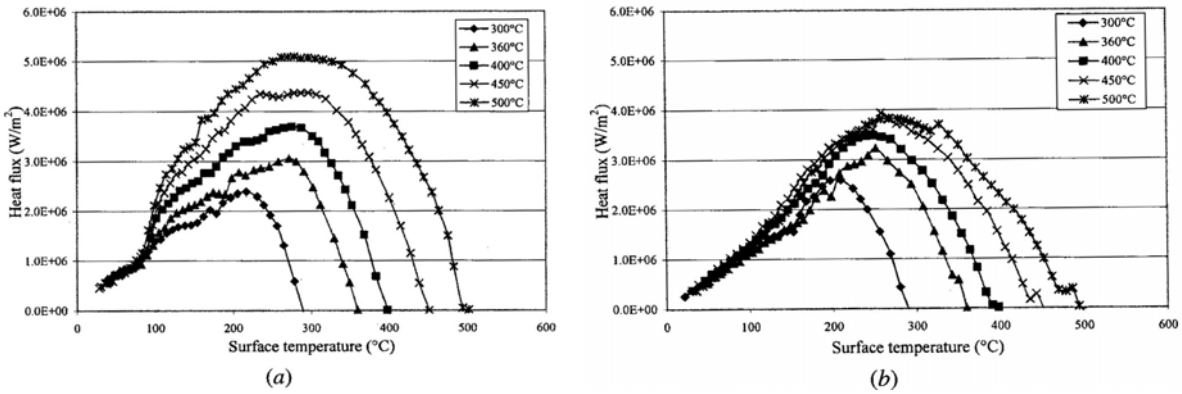

Figure 17 - Effect of initial sample temperature on calculated boiling curves[20] (as-cast AA5182, water flow rate = 0.38 ls^{-1}) for: (a) the impingement zone, and (b) the streaming zone.

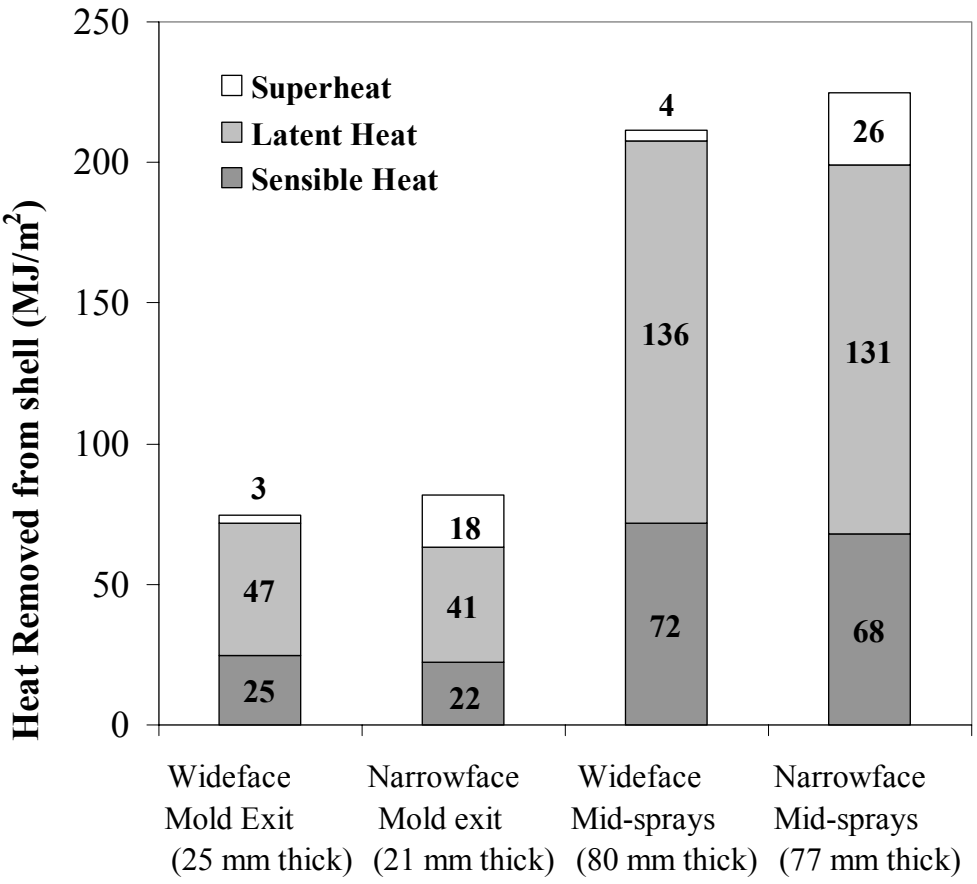

Figure 18 – Distribution of total heat removed from the shell at different locations during the continuous casting of steel[24].

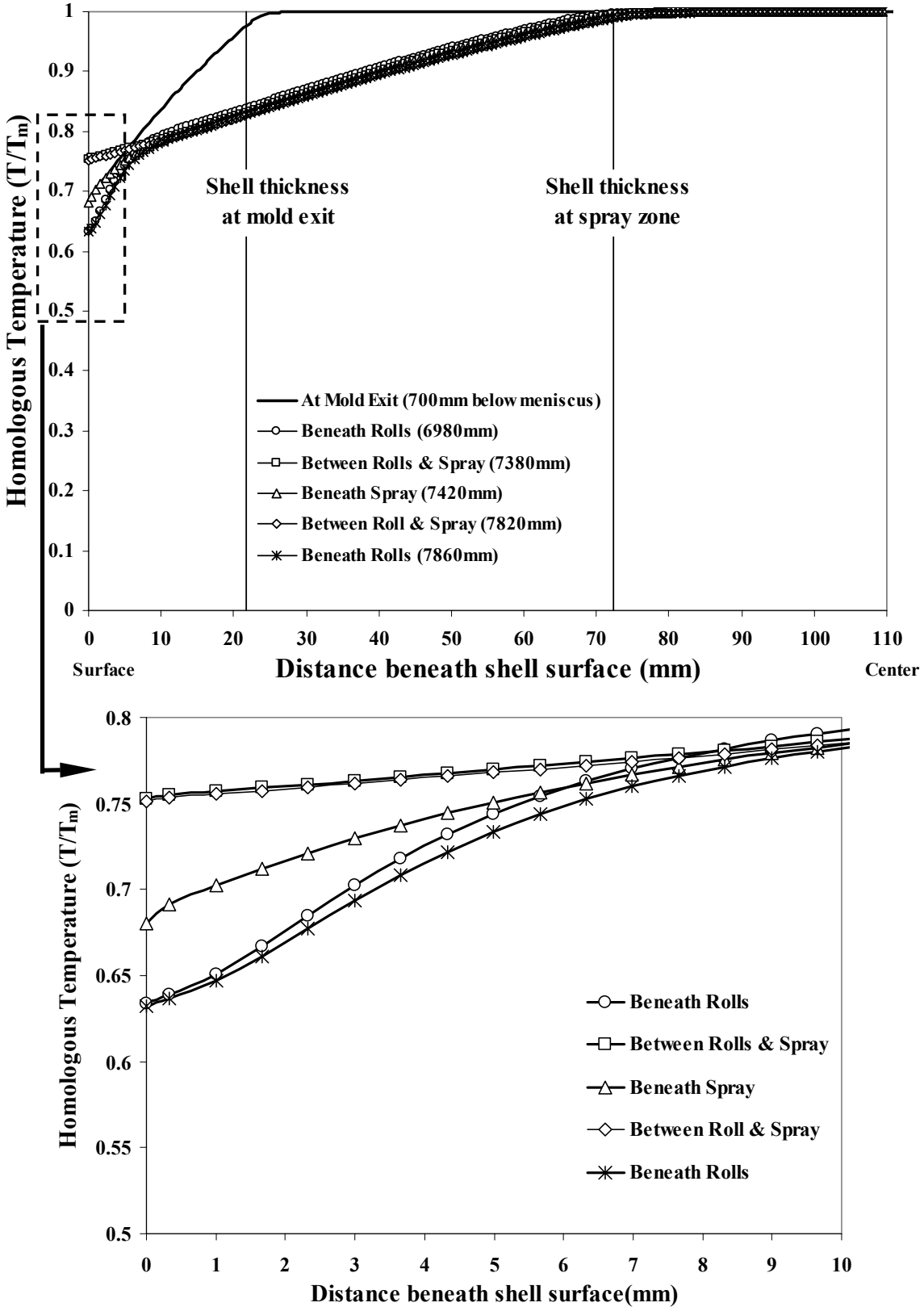

Figure 19 - Temperature profiles and shell thickness predicted in cross-sections through the strand taken at mold exit and during secondary cooling for continuous casting of steel[45].

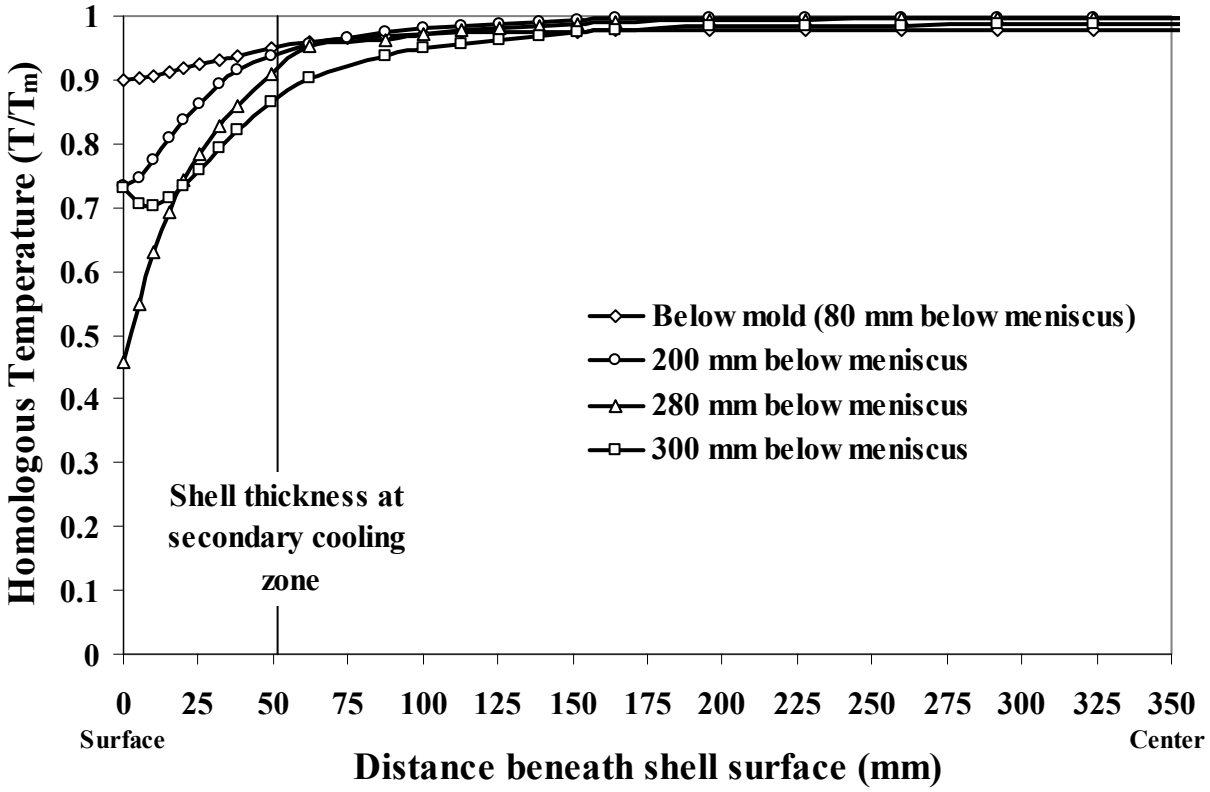

Figure 20 –Temperature profiles and shell thickness predicted in cross-sections through the ingot during secondary cooling taken ~375s after startup for D.C. casting of aluminum[2].

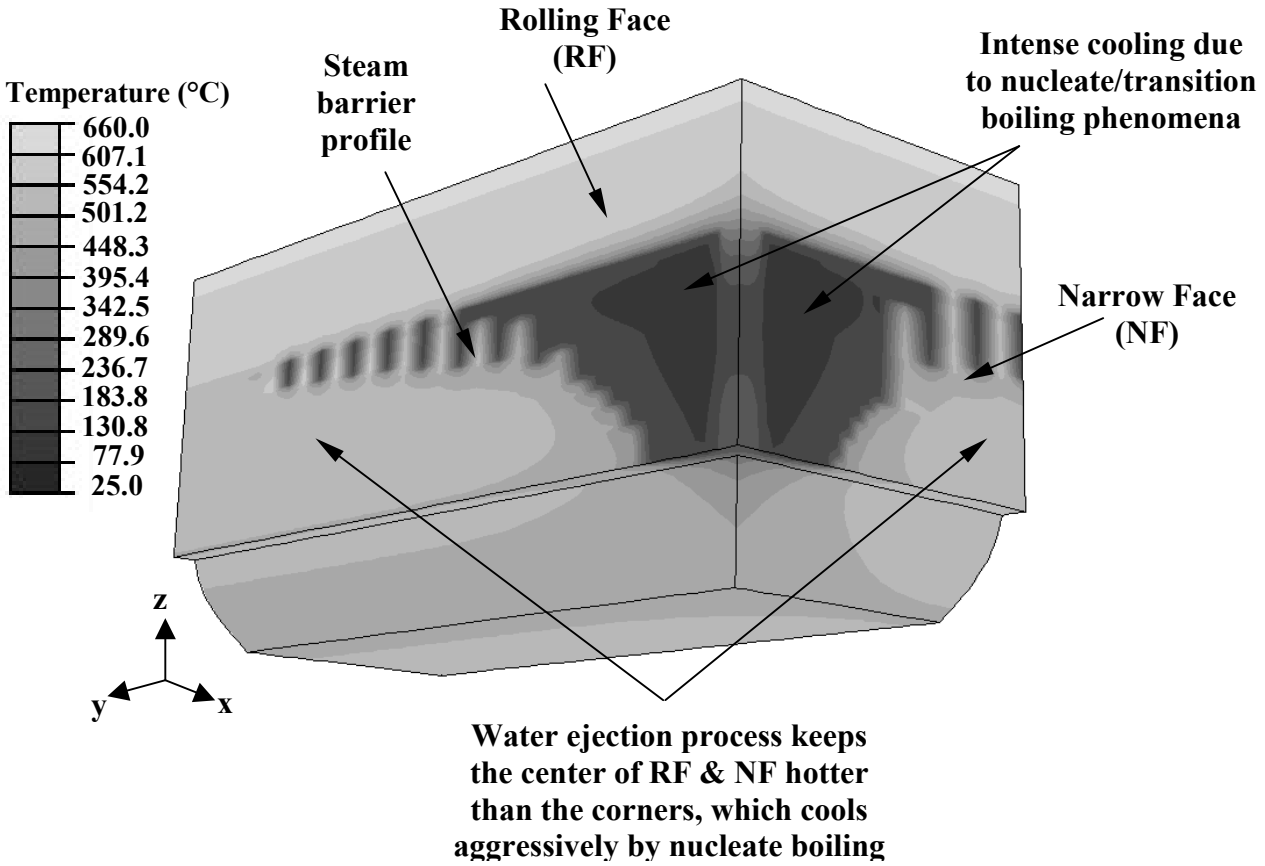

Figure 21 – Surface temperature contours on the narrow and rolling faces of a D.C. cast aluminum ingot at ~375s after start-up[2,5,80].

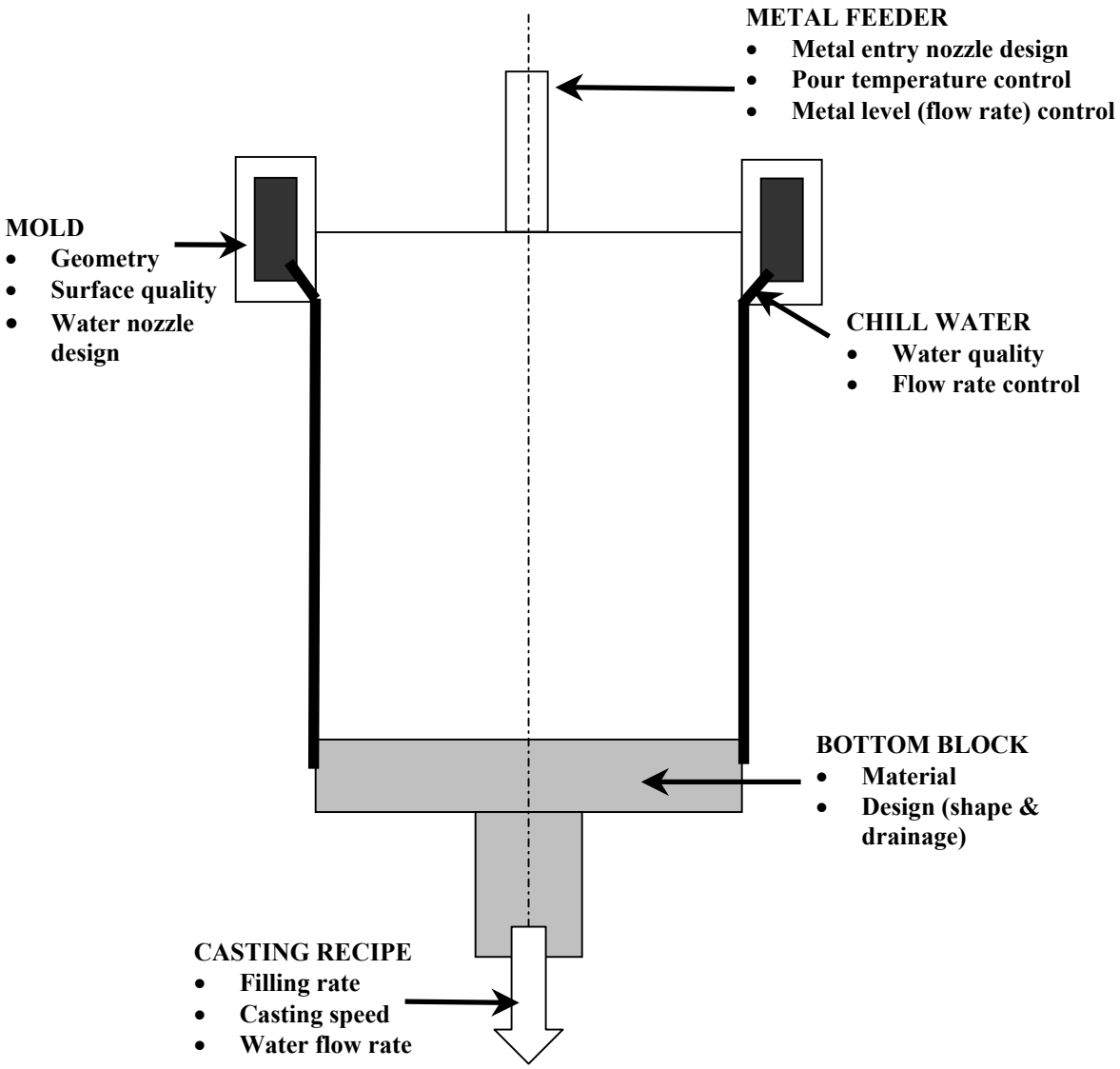

Figure 22 - Design and process parameters important to heat transfer during start-up of D.C. casting[87].